


























# ACCESS datasets for CMIP6: methodology and idealised experiments

C. Mackallah<sup>A,\*</sup> , M. A. Chamberlain<sup>B</sup> , R. M. Law<sup>A</sup> , M. Dix<sup>A</sup> , T. Ziehn<sup>A</sup> , D. Bi<sup>A</sup>, R. Bodman<sup>A,C</sup> , J. R. Brown<sup>C,D</sup> , P. Dobrohotoff<sup>A</sup> , K. Druken<sup>E</sup>, B. Evans<sup>E</sup>, I. N. Harman<sup>F</sup> , H. Hayashida<sup>G,D</sup> , R. Holmes<sup>H</sup> , A. E. Kiss<sup>I,D</sup> , A. Lenton<sup>B</sup> , Y. Liu<sup>E</sup>, S. Marsland<sup>A</sup> , K. Meissner<sup>J,D</sup> , L. Menviel<sup>J,K</sup> , S. O'Farrell<sup>A</sup> , H. A. Rashid<sup>A</sup> , S. Ridzwan<sup>E</sup>, A. Savita<sup>A,D,G</sup> , J. Srbinovsky<sup>A</sup>, A. Sullivan<sup>A</sup> , C. Trenham<sup>F</sup> , P. F. Vohralik<sup>L</sup>, Y.-P. Wang<sup>A</sup> , G. Williams<sup>M</sup> , M. T. Woodhouse<sup>A</sup>  and N. Yeung<sup>D,J</sup> 

For full list of author affiliations and declarations see end of paper

## \*Correspondence to:

C. Mackallah  
CSIRO Oceans and Atmosphere,  
Aspendale, Vic. 3195, Australia  
Email: [chloe.mackallah@csiro.au](mailto:chloe.mackallah@csiro.au)

Received: 16 December 2021

Accepted: 26 May 2022

Published: 14 July 2022

## Cite this:

Mackallah C *et al.* (2022)  
*Journal of Southern Hemisphere Earth  
Systems Science*  
72(2), 93–116. doi:[10.1071/ES21031](https://doi.org/10.1071/ES21031)

© 2022 The Author(s) (or their  
employer(s)). Published by  
CSIRO Publishing on behalf of BoM.  
This is an open access article distributed  
under the Creative Commons Attribution-  
NonCommercial-NoDerivatives 4.0  
International License ([CC BY-NC-ND](https://creativecommons.org/licenses/by-nc-nd/4.0/))

OPEN ACCESS

## ABSTRACT

The Australian Community Climate and Earth System Simulator (ACCESS) has contributed to the World Climate Research Programme's Coupled Model Intercomparison Project Phase 6 (CMIP6) using two fully coupled model versions (ACCESS-CM2 and ACCESS-ESM1.5) and two ocean–sea-ice model versions (1° and 0.25° resolution versions of ACCESS-OM2). The fully coupled models differ primarily in the configuration and version of their atmosphere components (including the aerosol scheme), with smaller differences in their sea-ice and land model versions. Additionally, ACCESS-ESM1.5 includes biogeochemistry in the land and ocean components and can be run with an interactive carbon cycle. CMIP6 comprises core experiments and associated thematic Model Intercomparison Projects (MIPs). This paper provides an overview of the CMIP6 submission, including the methods used for the preparation of input forcing datasets and the post-processing of model output, along with a comprehensive list of experiments performed, detailing their initialisation, duration, ensemble number and computational cost. A small selection of model output is presented, focusing on idealised experiments and their variants at global scale. Differences in the climate simulation of the two coupled models are highlighted. ACCESS-CM2 produces a larger equilibrium climate sensitivity (4.7°C) than ACCESS-ESM1.5 (3.9°C), likely a result of updated atmospheric parameterisation in recent versions of the atmospheric component of ACCESS-CM2. The idealised experiments run with ACCESS-ESM1.5 show that land and ocean carbon fluxes respond to both changing atmospheric CO<sub>2</sub> and to changing temperature. ACCESS data submitted to CMIP6 are available from the Earth System Grid Federation (<https://doi.org/10.22033/ESGF/CMIP6.2281> and <https://doi.org/10.22033/ESGF/CMIP6.2288>). The information provided in this paper should facilitate easier use of these significant datasets by the broader climate community.

**Keywords:** ACCESS, climate change, climate data, climate model evaluation, climate simulation, CMIP6, coupled climate model, Earth System Model.

## 1. Introduction

The Coupled Model Intercomparison Project (CMIP), overseen by the World Climate Research Programme (WCRP), endeavours to collate the results of a standardised set of experiments from global climate models developed at climate research organisations across the globe. The coordinated experiment design and implementation, along with the consolidated results of many different global climate models, allows for robust analysis and a deep investigation of the physical processes of the climate system and the biases inherent in numerical climate models. The current phase, CMIP6, consists of a base set of idealised experiments (known as the DECK; [Eyring \*et al.\* 2016](#)) and historical simulations

**Table 1.** Summary of modelling components for the four ACCESS global climate models submitted to CMIP6.

Component	ACCESS model			
	CM2	ESM1.5	OM2	OM2-025
Atmosphere	UM ver. 10.6 (N96, 85 levels)	UM ver. 7.3 (N96, 38 levels)	–	–
Aerosol	UKCA GLOMAP	UKCA CLASSIC	–	–
Land	CABLE 2.5	CABLE 2.4	–	–
Land carbon cycle	–	CASA–CNP	–	–
Ocean	MOM5 (1°)	MOM5 (1°)	MOM5 (1°)	MOM5 (1/4°)
Ocean biogeochemistry	–	WOMBAT	WOMBAT	–
Sea-ice	CICE 5.1.2	CICE 4.1	CICE 5.1.2	CICE 5.1.2

that modelling centres are required to perform in order to participate in CMIP6. In addition, ~322 different experiments have been designed across the 23 Model Intercomparison Projects (MIPs) endorsed by the World Climate Research Programme<sup>1</sup> (WCRP). These MIPs address a range of investigatory avenues – for example, exploring future climate projections under a range of socioeconomic scenarios (ScenarioMIP; O'Neill *et al.* 2016), and investigating the effects of removing carbon dioxide (CO<sub>2</sub>) from the atmosphere (CDRMIP; Keller *et al.* 2018).

Since the conclusion of CMIP5, two new iterations of the Australian Community Climate and Earth System Simulator (ACCESS), focusing on global climate, have been developed for the submission of simulation data to CMIP6. ACCESS-CM2 (Bi *et al.* 2020) simulates the physical climate with an updated atmospheric component, whereas ACCESS-ESM1.5 (Ziehn *et al.* 2020a) has been designed to simulate a fully-interactive carbon cycle; both models also have updated ocean and sea-ice components compared to the CMIP5-era versions of ACCESS. Although the two ACCESS models use broadly similar modelling components, ACCESS-CM2 uses newer versions of the atmospheric, land and sea-ice components, whereas ACCESS-ESM1.5 contains additional land and ocean biogeochemical components to facilitate the carbon cycle. Additionally, an ocean and sea-ice-only version of ACCESS-CM2 has been developed in partnership with the Consortium for Ocean–Sea-Ice Modelling in Australia (COSIMA) at three resolutions – ACCESS-OM2 (1° ocean), ACCESS-OM2-025 (0.25° ocean) and ACCESS-OM2-01 (0.1° ocean, which was not submitted to CMIP6), all referred to collectively as ‘ACCESS-OM2’ (Kiss *et al.* 2020). See Table 1 for details on the modelling components of each version of ACCESS. ACCESS has participated in the core CMIP/DECK and nine other MIPs, according to the needs of the Australian modelling community and the strengths of each model version.

One purpose of this paper is to document key details of the ACCESS submissions to CMIP6. Although there are well-defined protocols for each CMIP6 experiment, the differing

complexities of participating models and resources available to each modelling group mean that different choices (and sometimes compromises) are made as to how to meet the CMIP6 experimental specifications. Hence, one component of this paper (Section 1) documents these choices for the ACCESS models, including the spin-up that was performed before experiments were commenced and how the various forcing datasets were applied to each model configuration. A summary of the differences in model versions is provided, along with details of relevant model description and evaluation papers. Section 1 also provides a summary of all the experiments performed for CMIP6 with each ACCESS model, and the ACCESS datasets that are currently available on the Earth System Grid Federation (ESGF, which hosts the CMIP6 submissions across a number of data centres; Balaji *et al.* 2018). A description of the post-processing pipeline used to conform the model output and metadata to CMIP standards is provided, along with a brief analysis of the computational costs associated with the CMIP6 effort of our modelling group using prescribed metrics. The aim of this section is to provide sufficient information to support the reproducibility of experiments and further analysis of the existing ACCESS datasets.

A second aim of this paper (Section 2) is to provide a brief overview of some of the output from the DECK idealised experiments and related experiments from C4MIP (Jones *et al.* 2016) and CDRMIP (Keller *et al.* 2018). These experiments are used to characterise key features of a model's behaviour such as climate sensitivity, climate drift and overall performance against expected climate responses. The analysis focuses on global mean responses and notes how the simulated climate varies across the two ACCESS coupled models. Global carbon fluxes and related biogeochemical variables are presented for ACCESS-ESM1.5 simulations, with a focus on how changing atmospheric CO<sub>2</sub> and changing temperature affect the behaviour of the carbon cycle. This overview is intended as a springboard and to provide context for further studies, and to compare ACCESS simulations with other CMIP6 models in cases where multi-model studies have already been published.

<sup>1</sup><https://www.wcrp-climate.org/modelling-wgcm-mip-catalogue/modelling-wgcm-cmip6-endorsed-mips>

The paper concludes in Section 3 with some comments on the impact of the ACCESS submissions to CMIP6, whereas Section 3 directs the reader to repositories where the model codes and post-processed data are available.

## 2. Implementation of the CMIP6 protocol for ACCESS experiments

This section documents the steps required for the ACCESS models to participate in CMIP6, including a summary of the model configurations used, the experiments performed, the application of the forcing datasets for use with the ACCESS model and the post-processing required to meet CMIP6 standards.

### 2.1. Models

For its atmospheric component, ACCESS-CM2 uses the UK Met Office (UKMO) Unified Model (ver. 10.6, UM) GA7.1 configuration (Walters *et al.* 2019, MetUM-HadGEM3-GA7.1) with a vertical resolution of 85 levels and the GLOMAP-mode aerosol scheme (Mann *et al.* 2010). This is the same atmospheric configuration and resolution as the HadGEM3-GC31-LL and KACE-1-0-G CMIP6 submissions. ACCESS-ESM1.5 is based on an updated version of ACCESS1.3 (which was submitted to CMIP5; see Bi *et al.* 2013), and uses a UM (ver. 7.3) configuration that is close to GA1 (Bellouin *et al.* 2011a, HadGAM2) with 38 levels and the CLASSIC aerosol scheme (Bellouin *et al.* 2011b). Both are run at 'N96' horizontal resolution (1.875 longitude by 1.25 latitude) and make use of the Australian-developed land surface scheme CABLE (Community Atmosphere Biosphere Land Exchange; Kowalczyk *et al.* 2006, 2013), which is integrated into the UM atmosphere. The terrestrial carbon cycle is implemented in ACCESS-ESM1.5 using CASA-CNP (Wang *et al.* 2010), within CABLE, including accounting for the impact of nitrogen and phosphorus on the carbon cycle.

Additional components of ACCESS include the LANL CICE model for the sea-ice component (Hunke and Lipscomb 2010), and the NOAA/GFDL Modular Ocean Model (ver. 5, MOM5) for the ocean component at nominal 1° resolution (Griffies 2012). CICE and MOM5 are also the primary components of ACCESS-OM2, with 0.25° version of CICE and MOM5 used in ACCESS-OM2-025. ACCESS-ESM1.5 and ACCESS-OM2 (1° version only) also include the ocean biogeochemical modelling component WOMBAT (Whole Ocean Model of Biogeochemistry And Trophic-dynamics, Oke *et al.* 2013; Law *et al.* 2017). A tabulated breakdown of the differences between the ACCESS models used for CMIP6 can be found in Table 1.

More extensive documentation is available elsewhere. Bi *et al.* (2020) describes the ACCESS-CM2 configuration and the spin-up of the model. Climate drift is assessed and the model performance is evaluated including the mean state of

the ocean and aspects of climate variability. The simulated climate is compared with that of ACCESS1.3, as used in CMIP5. The climate of this model version has also been evaluated for an atmosphere-only (*amip*) simulation by Bodman *et al.* (2020), looking at both global and Australian metrics. Ziehn *et al.* (2020a) describes the ACCESS-ESM1.5 configuration including its performance compared with ACCESS-ESM1 (Law *et al.* 2017). The model is evaluated for climate and carbon cycle stability in the pre-industrial control simulation, whereas the later part of the historical simulation is used to evaluate against observations. Kiss *et al.* (2020) describes the ACCESS-OM2 configuration and provides extensive evaluation of simulations at three different resolutions. The ACCESS-OM2 configurations used for CMIP6 were updated relative to those described in Kiss *et al.* (2020) including, most notably, improved topography and updated forcing from JRA55-do ver. 1.3 to ver. 1.4. When WOMBAT was active in ACCESS-OM2, the biogeochemical parameters were identical to those described by Ziehn *et al.* (2020a) and used in ACCESS-ESM1.5.

### 2.2. Experiments and ensemble methodology

#### 2.2.1. Spin-up, DECK and historical experiments

Prior to beginning an official CMIP6 pre-industrial control experiment (*piControl*), a model must be initialised and spun-up under CMIP6 pre-industrial forcing conditions, in order to bring the model climate as closely into balance with the forcing as possible. The spin-up period of ACCESS-CM2 was 950 simulation years, during which several changes were made to the model, including the implementation of CABLE over the original land scheme JULES (Joint UK Land Environment Simulator; Best *et al.* 2011; Clark *et al.* 2011) and several bug fixes and tuning changes. The last 100 years of the ACCESS-CM2 spin-up were simulated using the final configuration of the model. The physical climate of ACCESS-ESM1.5 was spun-up over a period of 3000 simulation years with only minor changes and bug fixes applied during this time (with only very minor impacts on the climate trajectory), whereas the biogeochemical processes were integrated over the latter 1000 years of this spin-up. The last 600 years of spin-up represent the final ACCESS-ESM1.5 model configuration. OMIP-2 protocols do not require a spin-up period for the standard ocean-only experiments. Detailed descriptions of code changes and parameter tunings applied to the ACCESS models during their relative spin-up periods can be found in their respective model description papers: Bi *et al.* (2020) (ACCESS-CM2), Ziehn *et al.* (2020a) (ACCESS-ESM1.5) and Kiss *et al.* (2020) (ACCESS-OM2 and ACCESS-OM2-025).

The *piControl* experiment continues directly from the spin-up, with many experiments then branching from the first year of the *piControl* – designated year 0950 in ACCESS-CM2, and year 0101 in ACCESS-ESM1.5. The *piControl* underpins most other experiments by providing a baseline

with which to account for residual drift in the climate system that is not part of its response to forcings. The *piControl* experiment is part of the DECK, which also includes an idealised 1% per year CO<sub>2</sub> increase simulation (*1pctCO2*), an idealised simulation with an abrupt quadrupling of CO<sub>2</sub> concentration (*abrupt-4xCO2*), an Atmospheric Model Intercomparison Project simulation with prescribed sea surface temperatures (*amip*) and a *historical* simulation over the period 1850–2014. Furthermore, for Earth System Models<sup>2</sup> there is an additional *piControl* experiment and *historical* simulation required in which CO<sub>2</sub> emissions are prescribed, and a fully interactive carbon cycle simulated. In these experiments, *esm-piControl* and *esm-hist*, atmospheric CO<sub>2</sub> concentrations are calculated according to CO<sub>2</sub> fluxes between the atmosphere, ocean and land; as opposed to prescribing atmospheric CO<sub>2</sub> concentrations as in the *piControl* and *historical*.

### 2.2.2. Experiment characteristics and ensemble methodology

In addition to the DECK experiments, each MIP consists of Tier 1 (priority) and Tier 2 experiments. Each modelling group has chosen which experiments to complete with Tables 2–4 detailing the list of experiments performed for CMIP6 (as of April 2022) using ACCESS-CM2, ACCESS-ESM1.5 and ACCESS-OM2 respectively. The experiments are presented by MIP, with the start year referring to the first internal model year of the simulation, which is set to real dates where appropriate (e.g. in the *historical* simulation). For branched experiments that comprise only a single ensemble member, the branch year is usually the same as its start year (e.g. the ACCESS-ESM1.5 experiment *1pctCO2-cdr* begins at year 0241, having branched from *1pctCO2* at the end of year 0240), except where the internal year is set to a real date after branching (most commonly in the case of historical-based simulations; e.g. the ACCESS-ESM1.5 experiment *hist-bgc* branches from the *piControl* at year 0161, but the internal start date is set to 1850).

For experiments with multiple ensemble members, there are two different avenues of ensemble methodology: (i) new ensembles branching from a *piControl* or *esm-piControl*, and (ii) child ensembles branching from an existing parent ensemble. For case (i) – new ensembles that branch from a *piControl* (typically historical simulations) – the following methodology applies: each ensemble member of a child experiment is branched from a progressively advanced year of the *piControl* (or *esm-piControl*), and the ‘variant label’ of the child member is advanced by one ‘realisation’ (e.g. *r1i1p1f1* and *r2i1p1f1* are realisations one and two

respectively; see the CMIP6 Controlled Vocabulary<sup>3</sup> for details). The branch years of new ensembles are specified, where appropriate, in the right-hand column of Tables 2, 3; branch years are 50 years apart for ACCESS-CM2 and 20 years apart for ACCESS-ESM1.5. In cases where avenue (ii) applies, ensemble members of the child experiment will match those of its parent – for example, ensemble member three (*r3i1p1f1*) of *ssp126* was branched from ensemble member three (*r3i1p1f1*) of the *historical*. In these cases – primarily future scenario projections that branch from historical simulations – the ‘variant label’ of the child remains the same as the parent from which it was branched.

A second ACCESS-ESM1.5 *abrupt-4xCO2* simulation (*r2i1p1f1*) was run for 1000 years, for submission to the ongoing LongRunMIP<sup>4</sup> (Rugenstein et al. 2019), which is not an official CMIP activity. Furthermore, a large ensemble (defined as >10 realisations by Deser et al. (2020)) consisting of 40 members has been simulated with ACCESS-ESM1.5 for the *historical* and tier 1 ScenarioMIP experiments (*ssp126*, *ssp245*, *ssp370* and *ssp585*), along with a 30-member ensemble for the four experiments that were simulated from the CovidMIP activity (which sits within DAMIP and comprises a total of six experiments; Gillett et al. 2016; Jones et al. 2021). These large ensembles are available for use by the SMILE<sup>5</sup> (Single Model Initial-condition Large Ensemble) community, and will be investigated in more detail in papers currently in preparation. Work is also ongoing to expand the ACCESS-CM2 *historical* and ScenarioMIP ensembles, with the intention to produce a 10-member ensemble.

Three ACCESS-OM2 experiments (see Table 4) were contributed to OMIP through the OMIP-2 protocol (Griffies et al. 2016; Orr et al. 2017; Tsujino et al. 2020) forced by repeated 61-year (1958–2018) cycles of the Japanese atmospheric reanalysis (JRA55-do, ver. 1.4; Tsujino et al. 2018). The 1° ACCESS-OM2, including the ocean biogeochemistry component WOMBAT, ran both OMIP-2 experiments, *omip2* (six cycles) and *omip2-spinup* (six cycles after conducting 33 cycles as spin-up). The 0.25° ACCESS-OM2-025, without the ocean biogeochemistry component, was also used to run the *omip2* experiment (six cycles).

### 2.3. Forcings

Depending on the experiment, ACCESS requires time-varying forcings, including prescribed monthly solar forcing, greenhouse gases (GHGs), volcanic aerosol optical depth, aerosol chemistry emissions and ozone (Eyring et al. 2016). Land-use and land-cover forcing variations have also been implemented for ACCESS-ESM1.5. Most of the input forcing data were supplied either directly from CMIP6 by input4MIPs<sup>6</sup>

<sup>2</sup>That is, global climate models that simulate the carbon cycle, such as ACCESS-ESM1.5.

<sup>3</sup>[https://github.com/WCRP-CMIP/CMIP6\\_CVs](https://github.com/WCRP-CMIP/CMIP6_CVs)

<sup>4</sup><http://www.longrunmip.org/>

<sup>5</sup><https://large-ensemble.github.io/index>

<sup>6</sup><https://esgf-node.llnl.gov/projects/input4mips>

**Table 2.** ACCESS-CM2 (CSIRO-ARCCSS) experiments.

MIP	Experiment	Ensemble members	Start year	Parent	Branch year in parent
CMIP <sup>A</sup> (Dix <i>et al.</i> 2019a)	piControl	1 (500 years)	0950	piControl-spinup	
	amip	7	1979	no parent	
	1pctCO2	1	0950	piControl	
	abrupt-4xCO2	1	0950	piControl	
	historical	5	1850	piControl	0950/1000/1050/ 1100/1150
ScenarioMIP <sup>B</sup> (Dix <i>et al.</i> 2019b)	ssp126	5	2015	historical	
	ssp245	5	2015	historical	
	ssp370	5	2015	historical	
	ssp585	5	2015	historical	
	ssp534-over	1	2015	ssp585	
	ssp126 (extension)	1	2101	ssp126	
	ssp585 (extension)	1	2101	ssp585	
FAFMIP <sup>C</sup> (Savita <i>et al.</i> 2019)	faf-heat	1	0950	no parent	
	faf-water	1	0950	no parent	
	faf-stress	1	0950	no parent	
	faf-all	1	0950	no parent	
	faf-passiveheat	1	0950	no parent	
	faf-heat-NA0pct	1	0950	no parent	
	faf-heat-NA50pct	1	0950	no parent	
RFMIP <sup>D</sup> (Dix <i>et al.</i> 2020b)	piClim-control	1	0960	no parent	
	piClim-4xCO2	1	0960	piClim-control	
	piClim-aer	1	0960	piClim-control	
	piClim-ghg	1	0960	piClim-control	
	piClim-anthro	1	0960	piClim-control	
DAMIP <sup>E</sup> (Dix <i>et al.</i> 2020a)	hist-aer	3	1850	piControl	0950/1000/1050
	hist-GHG	3	1850	piControl	0950/1000/1050
	hist-nat	3	1850	piControl	0950/1000/1050

The *historical* ensemble is branched consecutively at 50-year intervals from *piControl*, starting at year 0950. The branch year in parent is only declared where it is different to the experiment start year. MIP footnotes direct the reader to experiment design papers and references under each MIP title cite the submitted data publications on the ESGF through Deutschen Klimarechenzentrum (DKRZ). The values in the final column indicate the branch years in the parent simulation for the various ensemble members.

<sup>A</sup>Eyring *et al.* (2016).

<sup>B</sup>O'Neill *et al.* (2016).

<sup>C</sup>Gregory *et al.* (2016).

<sup>D</sup>Pincus *et al.* (2016).

<sup>E</sup>Gillett *et al.* (2016).

(Meinshausen and Vogel 2016; Durack *et al.* 2018) or prepared by the UKMO for use in their HadGEM3-GC31-LL CMIP6 submission. Other forcings were determined as specified below.

Idealised experiments in CMIP6, such as *1pctCO2* and *abrupt-4xCO2*, largely follow the *piControl*, with historical data used in the *historical* and related experiments (such as

DAMIP; Gillett *et al.* 2016) and the *amip* simulation. Other MIPs provide or specify additional forcing data (e.g. ScenarioMIP; O'Neill *et al.* 2016) or protocols (e.g. RFMIP; Pincus *et al.* 2016).

In general, we adopted the same forcing files for ACCESS-CM2 as were used for HadGEM3-GC3.1 (Sellar *et al.* 2020), whereas ACCESS-ESM1.5 required further alterations to

**Table 3.** ACCESS-ESM1.5 (CSIRO) experiments.

MIP	Experiment	Ensemble members	Interactive CO <sub>2</sub>	Start year	Parent	Branch year in parent
CMIP (Ziehn et al. 2019c)	piControl	1 (1000 years)	–	0101	piControl-spinup	
	esm-piControl	1	Yes	0271	esm-piControl-spinup	
	amip	10	–	1979	no parent	
	lpctCO2	1	–	0101	piControl	
	abrupt-4xCO2	2 (1000 years)	–	0101	piControl	
	historical	40	–	1850	piControl	0161/0181 ...
	esm-hist	10	Yes	1850	esm-piControl	0321/0341 ...
ScenarioMIP (Ziehn et al. 2019d)	ssp126	40	–	2015	historical	
	ssp245	40	–	2015	historical	
	ssp370	40	–	2015	historical	
	ssp585	40	–	2015	historical	
	ssp126 (extension)	10	–	2101	ssp126	
	ssp585 (extension)	10	–	2101	ssp585	
C4MIP <sup>A</sup> (Ziehn et al. 2019a)	lpctCO2-bgc	1	–	0101	piControl	
	lpctCO2-rad	1	–	0101	piControl	
	hist-bgc	1	–	1850	piControl	0161
	ssp585-bgc	1	–	2015	hist-bgc	
	esm-ssp585	10	Yes	2015	esm-hist	
	esm-lpct-brch-1000PgC	1	Yes	0168	lpctCO2	
	esm-lpct-brch-750PgC	1	Yes	0154	lpctCO2	
	esm-lpct-brch-2000PgC	1	Yes	0216	lpctCO2	
CDRMIP <sup>B</sup> (Ziehn et al. 2019b)	lpctCO2-cdr	1	–	0241	lpctCO2	
	esm-pi-cdr-pulse	1	Yes	0271	esm-piControl	
	esm-pi-CO2pulse	1	Yes	0271	esm-piControl	
PMIP <sup>C</sup> (Yeung et al. 2019)	lig127k	1	–	0901	no parent	
	midHolocene	1	–	0501	no parent	
RFMIP (Ziehn et al. 2020c)	piClim-control	1	–	0121	no parent	
	piClim-4xCO2	1	–	0121	piClim-control	
	piClim-aer	1	–	0121	piClim-control	
	piClim-ghg	1	–	0121	piClim-control	
	piClim-anthro	1	–	0121	piClim-control	
	PiClim-lu	1	–	0121	piClim-control	
DAMIP <sup>D</sup> (Ziehn et al. 2020b)	hist-aer	3	–	1850	piControl	0161/0181/0201
	hist-GHG	3	–	1850	piControl	0161/0181/0201
	hist-nat	3	–	1850	piControl	0161/0181/0201
	ssp245-covid	30	–	2020	ssp245	
	ssp245-cov-strgreen	30	–	2020	ssp245	
	ssp245-cov-modgreen	30	–	2020	ssp245	

(Continued on next page)

**Table 3.** (Continued)

MIP	Experiment	Ensemble members	Interactive CO <sub>2</sub>	Start year	Parent	Branch year in parent
	ssp245-cov-fossil	30	–	2020	ssp245	
LUMIP <sup>E</sup> (Ziehn <i>et al.</i> 2021a)	hist-noLu	10	–	1850	piControl	0161/0181 ...
	ssp126-ssp370Lu	10	–	2015	historical	
	ssp370-ssp126Lu	10	–	2015	historical	
	esm-ssp585-ssp126Lu	10	Yes	2015	esm-hist	

Both *abrupt-4xCO2* realisations branch at year 0101 of *piControl*, but *r2ilplfl* ran for 1000 years. The *historical* (and *hist-noLu*) and *esm-hist* ensembles are branched consecutively at 20-year intervals from *piControl* and *esm-piControl*, starting from years 0161 and 0321. The branch year in parent is only declared where it is different to the experiment start year. MIP footnotes direct the reader to experiment design papers and references under each MIP title cite the submitted data publications on the ESGF though Deutschen Klimarechenzentrum (DKRZ). The values in the final column indicate the branch years in the parent simulation for the various ensemble members.

<sup>A</sup>Jones *et al.* (2016, 2019).

<sup>B</sup>Keller *et al.* (2018).

<sup>C</sup>Kageyama *et al.* (2018).

<sup>D</sup>Jones *et al.* (2021).

<sup>E</sup>Lawrence *et al.* (2016).

**Table 4.** ACCESS-OM2 (CSIRO-COSIMA) experiments.

MIP	Experiment	Model	Variant label	Start year	BGC included
OMIP <sup>A</sup>	omip2	ACCESS-OM2	rliplfl	0001	Yes
OMIP	omip2-spunup	ACCESS-OM2	rliplfl	2014	Yes
OMIP	omip2	ACCESS-OM2-025	rliplfl	0001	No

Start years here refer to those of the final processed datasets; internally the models cycle through six consecutive simulations of the period 1958–2018. MIP footnotes direct the reader to experiment design papers. For references to the submitted data publications on the ESGF though Deutschen Klimarechenzentrum (DKRZ), see Hayashida *et al.* (2021) (ACCESS-OM2) and Holmes *et al.* (2021) (ACCESS-OM2-025).

<sup>A</sup>Griffies *et al.* (2016), Orr *et al.* (2017), Tsujino *et al.* (2020).

input data, including interpolation to the HadGAM2 grid, or the use of separately prepared ancillary data as with land-use change forcings. The forcings used for the PMIP (Kageyama *et al.* 2018) experiments performed with the ACCESS-ESM1.5 (*lig127k* and *midHolocene*) follow the PMIP4 protocols (Otto-Bliesner *et al.* 2017).

### 2.3.1. Solar variability

For ACCESS-CM2, *piControl* (and associated experiments) solar forcing is based on a mean total solar insolation (TSI) value of 1361.0 W m<sup>-2</sup>, combined with a monthly time-varying spectral file that provides details for the solar cycle, based on the time-averaged mean conditions of the two solar cycles covering the years 1850–1873, and is derived from the recommended solar datasets for CMIP6 (Matthes *et al.* 2017).

For ACCESS-ESM1.5, the setup was slightly different. The model spin up was initiated prior to release of CMIP6 protocols, therefore both the spin-up and all idealised experiments, including the *piControl* were performed using the CMIP5 solar constant of 1365.65 W m<sup>-2</sup>, as it was in the CMIP5 versions of ACCESS. ACCESS-ESM1.5 does not utilise full spectral variations.

Historical and future scenario solar variability was based on the historical reconstructions of the 1850–2014 period, and projections of the 2015–2299 period, by Matthes *et al.* (2017). For ACCESS-ESM1.5, the CMIP6 TSI data were adjusted by a constant 4.9 W m<sup>-2</sup> offset in the historical and future simulations to match the CMIP5-style *piControl* setup (Ziehn *et al.* 2020a).

All experiments except PMIP use orbital parameters corresponding to the year 2000. For PMIP experiments, Earth's orbital parameters (eccentricity, longitude of perihelion and obliquity) were adjusted to the estimated values of the Last Interglacial and mid-Holocene periods (Berger and Loutre 1991; Otto-Bliesner *et al.* 2017). These orbital parameters modulate the magnitude, and seasonal and latitudinal distribution of the incoming solar radiation.

### 2.3.2. Stratospheric volcanic aerosol

Stratospheric volcanic aerosol optical depths (AODs), originating from explosive volcanic events, are determined from the zonal mean data of Arfeuille *et al.* (2014) and Thomason *et al.* (2018), with aerosol optical properties in the solar (shortwave) and terrestrial (longwave) spectrum. As per the CMIP6 protocols, a climatology of the 1850–2014

period was used for all idealised experiments and future scenarios past 2025, with a smooth transition occurring in 2015–2024 between the 2014 values and the climatology.

ACCESS-ESM1.5 and ACCESS-CM2 use different approaches for specifying stratospheric aerosols, with ACCESS-CM2 utilising AODs as a function of latitude, height and wavelength, as processed by the Easy Volcanic Aerosol module (Toohey et al. 2016). For ACCESS-ESM1.5, we derived AODs over four equal latitude bands from the simple 550 nm AOD data provided for use in CMIP6 (Ziehn et al. 2020a). A small offset was applied to account for the difference in the average AOD from CMIP6 and the CMIP5 data used for the ACCESS-ESM1-5 spin-up and *piControl*.

### 2.3.3. Well-mixed GHGs

The GHG concentrations are included in ACCESS models as globally uniform annual mass mixing ratios. ACCESS-CM2 uses CO<sub>2</sub>, methane (CH<sub>4</sub>), nitrous oxide (N<sub>2</sub>O), CFC12-eq and HFC134a-eq, with the latter two representing groups of chlorofluorocarbons (CFCs) and hydrofluorocarbons (HFCs) (Eyring et al. 2016). ACCESS-ESM1.5 uses CO<sub>2</sub>, CH<sub>4</sub>, N<sub>2</sub>O and separate values for CFC11, CFC12, CFC113, HCFC22, HFC125 and HFC134a, which together account for 98% of the change in the historical radiative forcing (Meinshausen et al. 2017). In the *piControl*, these values follow: CO<sub>2</sub> = 284.317 ppm, CH<sub>4</sub> = 808.25 ppb and N<sub>2</sub>O = 273.02 ppb. The GHG concentrations from Meinshausen et al. (2017) were used for the *historical* and related experiments (such as *amip*), whereas for all future scenarios the values from Meinshausen et al. (2020) were used. For PMIP experiments, the concentrations of CO<sub>2</sub>, CH<sub>4</sub> and N<sub>2</sub>O were adjusted to the estimated concentrations of the mid-Holocene and Last Interglacial (*lig127k*: CO<sub>2</sub> = 275 ppm, CH<sub>4</sub> = 685 ppb and N<sub>2</sub>O = 255 ppb; *midHolocene*: CO<sub>2</sub> = 264.4 ppm, CH<sub>4</sub> = 597 ppb and N<sub>2</sub>O = 262 ppb; Otto-Bliesner et al. 2017).

ACCESS-ESM1.5 was also used for CO<sub>2</sub> emissions-driven simulations (such as *esm-historical*) in interactive mode, with emissions prescribed by Hoesly et al. (2018). Emissions sources were combined and released from the surface, following interpolation to the ACCESS-ESM1.5 grid and scaling to ensure that total annual emissions agree with the CEDS project.<sup>7</sup> All other GHG concentrations are prescribed for ACCESS-ESM1.5 emissions-driven simulations.

### 2.3.4. Aerosol emissions (anthropogenic and natural)

Both ACCESS-CM2 and ACCESS-ESM1.5 use emissions of black carbon, organic carbon, sulfur dioxide, dimethyl sulfide (DMS) and sea salt for determining optical depths from tropospheric aerosol. Sources of carbon emissions include anthropogenic fossil-fuel and biofuel burning (Hoesly et al. 2018),

as well as the forest biomass burning emissions of van Marle et al. (2017), as per CMIP6 protocols. Sulfur dioxide emissions originate from both prescribed anthropogenic (Hoesly et al. 2018) and natural (volcanic degassing, calculated internally by climatology) sources which act as a precursor to secondary sulfate aerosol, along with DMS emissions, which are simulated interactively using prescribed seawater DMS. Sea salt emissions are also simulated interactively in both models. Biogenic and natural emissions are not supplied by CMIP6, and are implemented as in the setup of the UKMO CMIP6 models (Sellar et al. 2020), including a fixed monthly climatology of terpene emissions. Mineral dust is not included in the aerosol schemes of either model, and is simulated separately using the six-bin mass-based scheme of Woodward (2011).

In ACCESS-CM2, aerosol emissions are processed, and their evolution and interactions simulated, by the UKCA GLOMAP-mode module (Mann et al. 2010); whereas ACCESS-ESM1.5 uses the CLASSIC scheme of Bellouin et al. (2011b). Emission files were adopted from the setup of the UKMO GC3.1 model simulations, and were used directly in ACCESS-CM2, but ACCESS-ESM1.5 required regridding prior to use.

### 2.3.5. Ozone

Although some CMIP6 models simulate ozone, many prescribe ozone distributions. Both ACCESS configurations apply prescribed monthly ozone concentrations with ACCESS-CM2 using 3-D fields and ACCESS-ESM1.5 using zonal means. This input data originated from the ozone data sets of Morgenstern et al. (2017) for stratospheric ozone, and Checa-Garcia et al. (2018) for tropospheric ozone, which were interpolated from pressure levels to hybrid height coordinates by the UKMO (Sellar et al. 2020). For ACCESS-ESM1.5, further interpolation from 85 to 38 model levels was required.

In ACCESS-CM2 simulations (except for *piControl*), an additional calculation was applied at each simulation year in order to ensure that the prescribed ozone and model tropopause remain consistent as the tropopause height changes with temperature. The ozone redistribution scheme of Hardiman et al. (2019) redistributes excess tropospheric ozone concentrations into the stratosphere, while conserving global ozone mass. ACCESS-ESM1.5 has much lower vertical resolution about the tropopause and this adjustment would have much less effect and is not included.

### 2.3.6. Land use change and nitrogen deposition

ACCESS-ESM1.5 uses a simple land-use scheme which allows for annual changes in tile fractions, and reallocates carbon, nitrogen and phosphorus pools accordingly (Zhang et al. 2013; Ziehn et al. 2020a). Forcing data for changes in vegetation fractions were derived from the Land-Use Harmonisation 2 (LUH2) dataset (Hurtt et al. 2017), which

<sup>7</sup><http://www.globalchange.umd.edu/ceds/ceds-cmip6-data>



were mapped onto the CABLE plant functional types used in the model.

Nitrogen and phosphorus deposition forcings are used in all ACCESS-ESM1.5 simulations. Nitrogen deposition data are provided by CMIP6 (Jones *et al.* 2016), whereas phosphorus deposition data (not provided in CMIP6) were adopted from simulations of the predecessor of ACCESS-ESM1.5, ACCESS-ESM1, based on datasets used in Wang *et al.* 2010).

### 2.3.7. Atmosphere-only sea surface temperature and sea-ice cover forcings

Sea surface temperatures (SSTs) and sea-ice concentrations are prescribed in the atmosphere-only *amip* simulations of the DECK, the data for which were derived from the input4MIPs datasets of Durack and Taylor (2017), and interpolated to the UM model grid and N96 land-sea fractional mask by the UKMO.

These data were used in all ACCESS-ESM1.5 *amip* simulations, and in the first three ACCESS-CM2 *amip* ensemble members (r[1,2,3]i1p1f1), after which time it was discovered that a mismatch between the ACCESS-CM2 land-sea mask and that used to create the ancillary input files resulted in undefined SSTs at some coastal points, for which the model used a default SST of 273.1 K.<sup>8</sup> A corrected set of SST and sea-ice ancillary files were used for an additional set of three *amip* simulations with ACCESS-CM2, which were assigned the variant strings r[1,2,3]i1p1f2. We note here that the *amip* evaluation by Bodman *et al.* (2020) included only the initial set of ACCESS-CM2 *amip* ensemble members (r[1,2,3]i1p1f1). ACCESS-ESM1.5 simulations were not affected.

The SST and sea-ice concentrations were also prescribed in all RFMIP experiments. Climatologies were calculated from the first 50 years of the *piControl* experiment of each model. These were then interpolated to daily values, and adjusted following the AMIP II boundary condition calculation of Taylor *et al.* (2000) to ensure that the interpolated monthly means match the original climatology. No issues arose from these ancillary files, because they were internally consistent with each of the models and their associated land-sea masks.

## 2.4. Post-processing

The creation of datasets suitable for publication to the ESGF requires significant resources. An outline of the process for ACCESS datasets is provided here. The raw model output from the UM atmospheric component (along with the

CABLE land component output) of ACCESS exists in a binary file format (known as ‘Fieldsfiles’ or the ‘PP-format’<sup>9</sup>); and is converted to netCDF4 using the Python package *Iris* (Met Office 2020) as a first step in the post-processing pipeline (noting that the first several CMIP6 production simulations used *cdms2*<sup>10</sup> instead). All other components of ACCESS natively produce model output in netCDF format.

A Python-based software package, referred to as the ‘ACCESS Post-Processor ver. 4.0’ (APP4; Mackallah *et al.* 2022), has been developed to enable the generation of CMIP6 data using ACCESS model output, and is based on an earlier version of the APP that was used for the ACCESS submission to CMIP5 (Collier and Uhe 2012; Uhe *et al.* 2012). APP4 uses a *python2.7* environment and *cdms2* to extract and prepare the relevant fields from the model output, and relies on PCMDI’s ‘Climate Model Output Rewriter’ (CMOR ver. 3.4<sup>11</sup>; Nadeau *et al.* 2016) to create final data products, ensuring that they adhere to CMIP6 quality standards and follow the CMIP6 data reference syntax<sup>12</sup> (DRS) and CF metadata conventions.<sup>13</sup> Note that the *model\_id* for ACCESS-ESM1.5 is ACCESS-ESM1-5, this is reflected in all directory and file names. Primary inputs include an experiment-specific data request (created using the *dreqPy* tool ver. 01.00.31, Jukes *et al.* 2020), the CMIP6 CMOR Tables,<sup>14</sup> which define the controlled vocabulary and conventions, and an internally created mapping file that specifies how each CMIP6 variable is generated from the existing fields in the ACCESS model output. Reproducibility and code availability are detailed in Section 3.

Key variables that require significant treatment beyond simple arithmetical calculations include overturning circulations and streamfunctions (e.g. *msftyz*), ocean and sea-ice transports (e.g. *mfo*), and sea-ice extents, volumes and areas (e.g. *siextentn*). These are performed by APP4 internally with Python functions, prior to the use of CMOR. Furthermore, many variables require minor manipulations such as averaging over spatial, temporal or tiled dimensions (e.g. most annual variables are based on monthly data), unit conversions (performed by CMOR where possible), masking or the filling of missing values, and the calculation of climatologies. Basic quality checking of metadata is performed using CMOR’s *PrePARE* tool, along with automatically generated plots to identify spurious and missing data.

As of 11 April 2022, 37 028 ACCESS-CM2 datasets, 265 166 ACCESS-ESM1.5<sup>15</sup> datasets and 822 ACCESS-OM2 datasets have been submitted to the ESGF,<sup>16</sup> where each

<sup>8</sup>see errata: <https://errata.es-doc.org/static/view.html?uid=5fda6ba1-3b14-38a1-94b9-22a09ad7e92e>

<sup>9</sup>see <https://help.ceda.ac.uk/article/4424-pp-binary-format>

<sup>10</sup><https://cdms.readthedocs.io/en/latest/cdms2.html>

<sup>11</sup><https://cmor.llnl.gov>

<sup>12</sup>see <https://goo.gl/v1drZl> ‘CMIP6 Global Attributes, DRS, Filenames, Directory Structure, and CV’s’.

<sup>13</sup><https://pcmdi.llnl.gov/CMIP6/Guide/modelers.html>

<sup>14</sup><https://github.com/PCMDI/cmip6-cmor-tables>

<sup>15</sup>ACCESS-ESM1.5 is spelled as ACCESS-ESM1-5 on the ESGF in order to follow CMIP6 conventions concerning model naming.

<sup>16</sup><http://esgf-ui.cmcc.it/esgf-dashboard-ui/data-archiveCMIP6.html>

**Table 5.** Computational performance of ACCESS models following CPMIP (Balaji et al. 2017) metrics.

Metric	ACCESS-CM2	ACCESS-ESM1.5	ACCESS-OM2	ACCESS-OM2-025
Resolution	$7.9 \times 10^6$	$6.6 \times 10^6$	$5.5 \times 10^6$	$7.9 \times 10^7$
Complexity	48	41	36	26
SYPD	5.5	20	53	12
CHSY	2900	500	120	3600
Coupling cost (%)	7	12	–	–
Data output cost (%)	2	2	11	33
Data intensity	0.005–0.018	0.025	0.05	0.02

All statistics from simulations on NCI's Gadi HPC system. SYPD, simulated years per day; CHSY, core hours per simulated year.

dataset is a single version of an individual variable at a given time frequency for each ensemble member. Version strings (e.g. ver. 20191225) contain the date on which the dataset was generated, with new versions being generated in the case of retraction and republication (see the CMIP Errata service for details on all ACCESS dataset retractions<sup>17</sup>). There have been DOIs minted for datasets grouped by MIP and the relevant citations are noted in Tables 2–4.

## 2.5. Computational costs and CPMIP metrics

All simulations with ACCESS models for CMIP6 were performed on the High Performance Computing (HPC) systems of the National Computational Infrastructure (NCI) at the Australian National University. The supercomputer Raijin was used for the first several ACCESS simulations performed, including the *piControl-spinup* and most of the DECK experiments; and for the *historical* and ScenarioMIP experiments, the first realisation of ACCESS-CM2 and first three realisations of ACCESS-ESM1.5. All later simulations were run on its replacement system Gadi. Tests with ensembles of fifty 1-year simulations showed that the climates simulated on the two machines were indistinguishable. Although not bit-wise reproducible, the results were consistent across all variables to the same level of internal climate variability seen among ensemble members, indicating that the model simulations were consistent across HPC systems.

ACCESS-CM2 simulations were performed in suites developed using the Rose engine<sup>18</sup> and scheduled using the Cylc workflow engine.<sup>19</sup> Most ACCESS-ESM1.5 simulations were configured and scheduled with scripts held at NCI, with the exception of PMIP experiments which were run using the *payu* framework developed by the ARC Centre of Excellence for Climate Extremes (CLEX). The *payu* framework was also used for the ACCESS-OM2 simulations. Code availability is detailed in Section 5.

Following an assessment of the computational performance of CMIP6 Earth System Models by Balaji et al. (2017),

we present the performance of the ACCESS models against the metrics described by the Computational Performance MIP (CPMIP) project in Table 5. Values are taken from simulations performed on NCI's Gadi HPC system (Cascade Lake nodes). The CPMIP resolution is the total number of 3-D grid points, and in the coupled model configurations is dominated by the ocean, so ACCESS-CM2 and ACCESS-ESM1.5 have quite similar values. However, the extra complexity of the atmospheric physics means that the atmosphere dominates the computational cost and limits the scaling in ACCESS-CM2. Therefore there is no close relation between resolution and cost in these metrics. Complexity (number of prognostic variables) is larger for ACCESS-CM2 than ACCESS-ESM1.5 because of the more sophisticated atmospheric chemistry and aerosol scheme. It is larger for ACCESS-OM2 compared to ACCESS-OM2-025 because only the former includes the ocean biogeochemical component WOMBAT. For ACCESS-CM2 and ACCESS-ESM1.5, data intensity (measured in gigabytes per compute hour) and data output cost depend on whether sub-daily data are saved from the atmospheric component; values presented are from a simulation in which sub-daily data were not saved.

## 3. Results from idealised experiments

In this section we present a range of metrics from different components of the climate system, both physical and biogeochemical, from the two fully coupled models ACCESS-CM2 and ACCESS-ESM1.5. The ocean-only ACCESS-OM2 results will be presented in a separate paper, in preparation. These metrics show the stability of the models in control experiments and also the responses to perturbations over a span of timescales in idealised climate warming scenarios. The figures that follow demonstrate that the impacts of these perturbations vary widely across the climate system; some components can be sensitive to a particular perturbation

<sup>17</sup><https://errata.es-doc.org/static/index.html>

<sup>18</sup><https://metomi.github.io/rose>

<sup>19</sup><https://cylc.github.io/cylc>

while insensitive to others. Some impacts are persistent but others are relatively transient. There is insufficient space here for a detailed study of the simulated fields or their responses to climate change. Rather, the overview here provides context for and motivates further analysis. The mean climate states and drifts in the models are already reported in their respective model description papers (Bi *et al.* 2020; Ziehn *et al.* 2020a), so the focus here is on comparing their behaviour. Climate responses from historical and future projections from ACCESS models are not covered here but where there is relevant evaluation as part of a multimodel study, this is cited in the discussions below.

This overview uses only a small selection of the variables submitted to CMIP6 (e.g. Dix *et al.* 2019a; Ziehn *et al.* 2019c) and their descriptions are listed in Table 6. The global mean physical climate variables used for ACCESS-CM2 and ACCESS-ESM1.5 are near-surface air temperature (*tas*), top of atmosphere (TOA) net energy balance down (*rsdt* – *rsut* – *rlut*), sea-ice area (*siarean* + *siareas*) and ocean temperature (*thetaoga*). For ACCESS-ESM1.5, the global biogeochemical (BGC) metrics used are net land carbon flux (*nbp*, positive into land), land net primary productivity (*npp*), net ocean carbon flux

(*fgco2*, positive into ocean), ocean productivity (*intpp*), ocean O<sub>2</sub> flux (*fgo2*, positive into ocean), ocean surface acidity (derived from *dissic*, *talk* and equilibrium constants) and global atmospheric CO<sub>2</sub> mixing ratio (*co23D*).

We first discuss the control simulations and then the climate response for the experiments where CO<sub>2</sub> is quadrupled (*abrupt-4xCO2*) or increases by 1% per year (*1pctCO2*). Effective radiative forcings calculated using RFMIP experiments (Pincus *et al.* 2016) are also presented. This is followed by C4MIP (Jones *et al.* 2016) and CDRMIP (Keller *et al.* 2018) experiments that are based on the idealised experiments and have been run with ACCESS-ESM1.5. Selected BGC fields are then discussed for the idealised experiments and their variants.

### 3.1. Control simulations

The *piControl* simulation has been run for 500 years with ACCESS-CM2, and 1000 years with ACCESS-ESM1.5. The longer *piControl* run for ACCESS-ESM1.5 was required for the long reversibility experiment in CDRMIP and the extended length (1000 years) run for *abrupt-4xCO2* (r2i1p1f1).

**Table 6.** List of CMIP6 variables used in the present analysis.

CMIP6 variable (units) <sup>A</sup>	CF_standard_name <sup>B</sup>	Description
tas(K)	<i>air_temperature</i>	Near-surface (usually 2 m) air temperature.
rsdt(W m <sup>-2</sup> )	<i>toa_incoming_shortwave_flux</i>	Shortwave radiation incident at the top of the atmosphere.
rsut(W m <sup>-2</sup> )	<i>toa_outgoing_shortwave_flux</i>	Outgoing shortwave radiation at the top of the atmosphere.
rlut(W m <sup>-2</sup> )	<i>toa_outgoing_longwave_flux</i>	Outgoing longwave radiation at the top of the atmosphere.
siarean(10 <sup>6</sup> km <sup>2</sup> )	<i>sea_ice_area</i>	Total area of sea ice in the northern hemisphere.
siareas(10 <sup>6</sup> km <sup>2</sup> )	<i>sea_ice_area</i>	Total area of sea ice in the southern hemisphere.
thetaoga(°C)	<i>sea_water_potential_temperature</i>	Global average sea water potential temperature.
nbp(kg m <sup>-2</sup> s <sup>-1</sup> )	<i>surface_net_downward_mass_flux_of_carbon_dioxide_expressed_as_carbon_due_to_all_land_processes</i>	Net mass flux of carbon from atmosphere into land, calculated as photosynthesis minus the sum of plant and soil respiration, carbon fluxes from fire, harvest, grazing and land use change.
npp(kg m <sup>-2</sup> s <sup>-1</sup> )	<i>net_primary_productivity_of_biomass_expressed_as_carbon</i>	Excess of gross primary production (rate of synthesis of biomass from inorganic precursors) by autotrophs.
fgco2(kg m <sup>-2</sup> s <sup>-1</sup> )	<i>surface_downward_mass_flux_of_carbon_dioxide_expressed_as_carbon</i>	Gas exchange flux of CO <sub>2</sub> (positive into ocean).
fgo2(mol m <sup>-2</sup> s <sup>-1</sup> )	<i>surface_downward_mole_flux_of_molecular_oxygen</i>	Gas exchange flux of O <sub>2</sub> (positive into ocean).
intpp(mol m <sup>-2</sup> s <sup>-1</sup> )	<i>net_primary_mole_productivity_of_biomass_expressed_as_carbon_by_phytoplankton</i>	Vertically integrated total primary (organic carbon) production by phytoplankton.
dissic(mol m <sup>-3</sup> )	<i>mole_concentration_of_dissolved_inorganic_carbon_in_sea_water</i>	Dissolved inorganic carbon (CO <sub>3</sub> + HCO <sub>3</sub> + H <sub>2</sub> CO <sub>3</sub> ) concentration.
talk(mol m <sup>-3</sup> )	<i>sea_water_alkalinity_expressed_as_mole_equivalent</i>	Total alkalinity equivalent concentration (including carbonate, nitrogen, silicate and borate components).
co23D(kg kg <sup>-1</sup> )	<i>mass_fraction_of_carbon_dioxide_tracer_in_air</i>	3-D field of model simulated atmospheric CO <sub>2</sub> mass mixing ratio on model levels.

<sup>A</sup><https://clipc-services.ceda.ac.uk/dreq/index/var.html>

<sup>B</sup><https://cfconventions.org/standard-names.html>

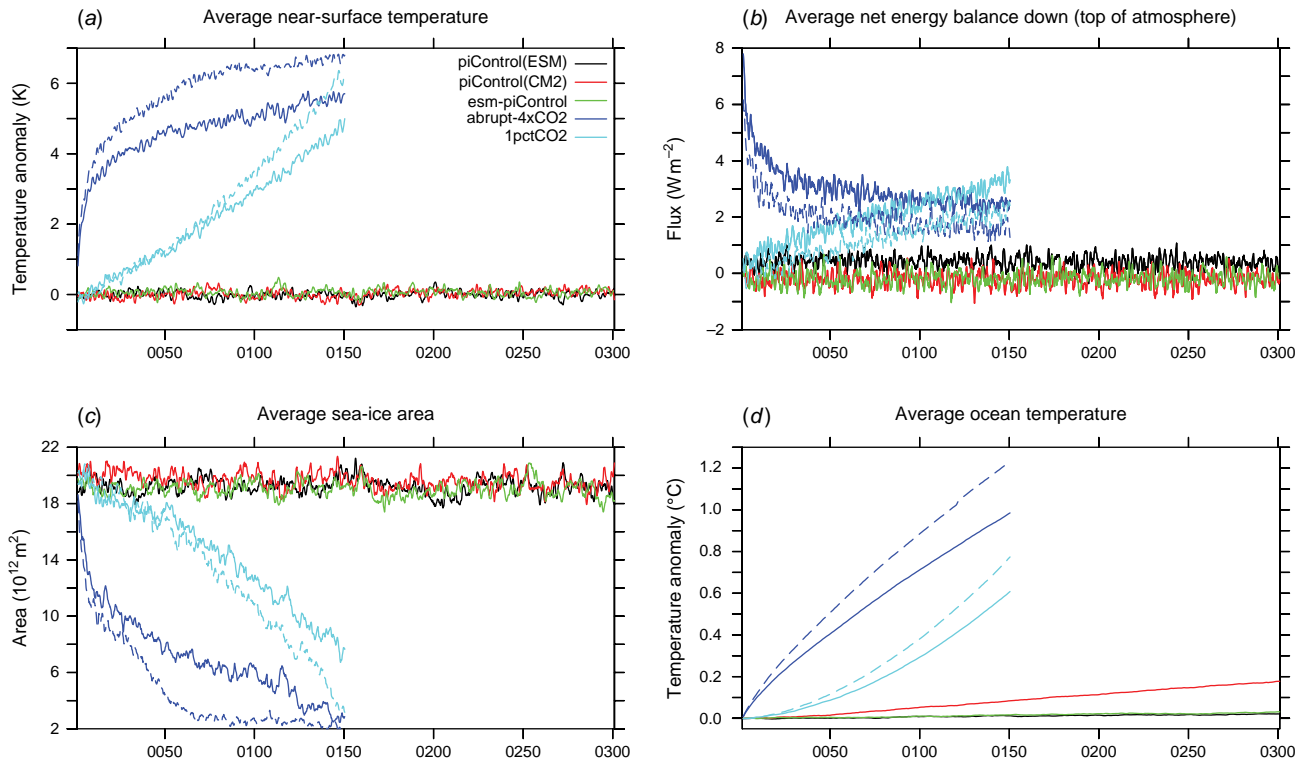


**Fig. 1.** Global physical climate metrics from CMIP idealised experiments. Trends of anomalies in average global surface temperature (top left), net radiative energy flux (top right), sea-ice cover (bottom left) and anomalies in average total ocean temperature (bottom right), from idealised CMIP6 experiments with ACCESS-ESM1.5 (solid lines for transient experiments, black for *piControl* and green for *esm-piControl*) and ACCESS-CM2 (dashed lines for transient experiments, red for *piControl*). 12-month boxcar filters have been applied to all metrics.

Results from the first 300 years of the *piControl* of both models are shown in Fig. 1.

Temperatures are plotted as anomalies relative to the first decade of the respective controls. There is a difference (not shown) of  $\sim 0.6$  K in the global near-surface air temperature (*tas*) of the two models at the start of their respective control simulations (years 0950 and 0101 for ACCESS-CM2 and ACCESS-ESM1.5 respectively), with ACCESS-ESM1.5 being warmer; this is likely due to the longer spin-up of ACCESS-ESM1.5. There is a small drift in global *tas* in both models; a linear fit gives  $4.99 \times 10^{-4} \text{ K year}^{-1}$  for ACCESS-CM2 (500 years) and  $6.54 \times 10^{-5} \text{ K year}^{-1}$  for ACCESS-ESM1.5 (1000 years). These drifts are close to those of global ocean temperatures (*thetaoga*, Fig. 1d) of  $5.51 \times 10^{-4} \text{ K year}^{-1}$  for ACCESS-CM2 and  $6.39 \times 10^{-5} \text{ K year}^{-1}$  for ACCESS-ESM1.5. The drift in total ocean temperature of ACCESS-CM2 is approximately twice the magnitude of an earlier version of ACCESS, ACCESS-1.3, and has the opposite sign (Bi et al. 2020); the drift is substantially less in ACCESS-ESM1.5 due to the long spin-up. Drifts in coupled models are common, and the ACCESS models' drifts are similar to other CMIP6 models (Irving et al. 2021).

As reported in Ziehn et al. (2020a), the drift in ACCESS-ESM1.5 does not correspond with the TOA net radiation

imbalance (Fig. 1b), which shows an energy loss of  $0.25 \text{ W m}^{-2}$ . Approximately 40% of the global energy imbalance is contributed by CABLE, but the source of the remainder is not known (Ziehn et al. 2020a). Bi et al. (2020) discuss the ACCESS-CM2 TOA radiation imbalance in relation to the total ocean warming, noting that 87% of the ocean's net gain in energy is due to the TOA imbalance, with the remainder attributed to a lack of energy conservation. These discrepancies in energy conservation are similar to other CMIP6 models (Irving et al. 2021). Fig. 1c also shows global sea-ice area which is relatively stable at  $\sim 20 \times 10^{12} \text{ m}^2$  for the *piControl* run from both models, with drifts of less than  $-0.003 \times 10^{12} \text{ m}^2 \text{ year}^{-1}$ .

A second control run, *esm-piControl*, is required for models with an interactive carbon cycle such as ACCESS-ESM1.5. In this simulation the atmospheric  $\text{CO}_2$  is not fixed but evolves depending on the net land and ocean carbon fluxes. For a control run, these fluxes should be close to zero (globally and averaged over decades) so that the atmospheric  $\text{CO}_2$  does not drift. The 500-year *esm-piControl* run starts after 170 years of spin-up with freely evolving atmospheric  $\text{CO}_2$ , with the spin-up starting from the initial year of the standard *piControl*. The global mean surface-layer  $\text{CO}_2$  (Fig. 2) drifts slightly in the *esm-piControl* run ( $1 \text{ ppm century}^{-1}$ ) due to

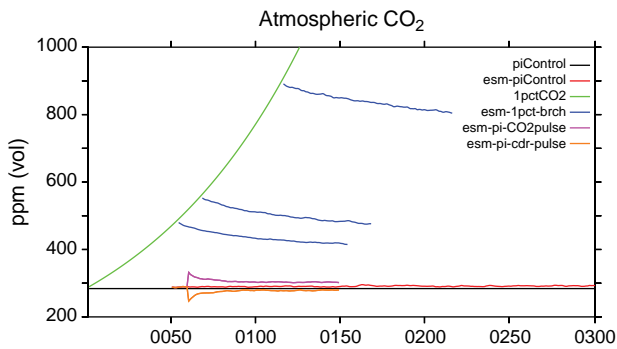


**Fig. 2.** Global average surface-layer CO<sub>2</sub> from emission driven experiments with ACCESS-ESM1.5: *esm-piControl*, ZECMIP and CDRMIP pulse experiments. For reference, *piControl* and *1pctCO2* are included. 12-month boxcar filters have been applied to all metrics.

global mean land and ocean carbon fluxes to the atmosphere of  $-0.03$  and  $0.05$  Pg C year<sup>-1</sup> respectively.

This drift is well within the guidelines for C4MIP of less than 5 ppm century<sup>-1</sup> (Jones *et al.* 2016). The drift in CO<sub>2</sub> leads to a larger temperature drift ( $2.26 \times 10^{-4}$  K year<sup>-1</sup>) in the *esm-piControl* compared to the *piControl* but this is still very small (as seen in Fig. 1a).

### 3.2. Climate from idealised experiments

The *abrupt-4xCO2* and *1pctCO2* simulations see large increases in atmospheric CO<sub>2</sub>, producing an increase in temperature, a reduction in sea-ice area and a positive TOA energy balance. Results from these simulations with ACCESS are shown in Fig. 1, with the greater warming in ACCESS-CM2 over ACCESS-ESM1.5 due largely to the different atmospheric configurations. These simulations can be used to calculate a model's equilibrium climate sensitivity (ECS, based on *abrupt-4xCO2*; Gregory *et al.* 2004) and transient climate response (TCR, based on *1pctCO2*). For ACCESS-CM2, the ECS and TCR are 4.7 and 2.1°C respectively (Meehl *et al.* 2020), whereas ACCESS-ESM1.5 has an ECS of 3.9 and TCR of 2.0°C (Ziehn *et al.* 2020a), which is similar to the climate sensitivities of ACCESS1.0 and ACCESS1.3 (3.6 and 3.9°C respectively; Zelinka *et al.* 2020) which were submitted to CMIP5.

Both the mean and spread of ECS values among models submitted to CMIP6 are significantly higher than those in CMIP5 (Grose *et al.* 2020). Furthermore, several CMIP6 models simulate climate responses that do not match ECS estimates from independent assessments using multiple lines of evidence; for example, Sherwood *et al.* (2020) determined a likely ECS range of 2.3–4.5 K, based on historical and palaeoclimatological records. This overall increase in CMIP6 ECS is largely driven by a subset of models with new or updated physics, such as ACCESS-CM2, which tend to have high ECS values. An investigation of 50 CMIP6 models by Zelinka *et al.* (2020), in which 16 were found to have an ECS higher than ACCESS-CM2 (including the Met Office

models), demonstrated that these ECS increases are primarily due to the representation of cloud microphysics. This provides an explanation as to why ACCESS-CM2 saw the increase but ACCESS-ESM1.5 did not, since the atmospheric components in ACCESS-CM2 have diverged the most since the ACCESS1.3 configuration in CMIP5. Interestingly, the KACE-1-0-G model (Lee *et al.* 2020) simulated an ECS of 4.5°C (Meehl *et al.* 2020), very similar to ACCESS-CM2; these two models share the same atmosphere (UM ver. 10.6) and similar ocean model (MOM4.1 in KACE-1-0-G, and MOM5 in ACCESS-CM2). By contrast, HadGEM3-GC31-LL uses the same atmosphere but a different ocean (NEMO ver. 3.6; Storkey *et al.* 2018), and simulated a significantly higher ECS (ECS = 5.5°C; Senior *et al.* 2020). This suggests that the ocean and sea-ice components may play a significant role in ECS; however, further investigation is required to understand this complexity.

The larger climate sensitivity of ACCESS-CM2 also shows up in the larger TOA energy imbalance from the increase in atmospheric CO<sub>2</sub>; this is likely due to a GA7.0 update in the representation of CO<sub>2</sub> absorption, resulting in a higher CO<sub>2</sub> effective radiative forcing (ERF; discussed further below in relation to RFMIP). As expected, the larger temperature increase in ACCESS-CM2 leads to a larger loss of sea ice, with rapid initial sea-ice loss in both models for the *abrupt-4xCO2* case. ACCESS-CM2 shows a further period of rapid loss around years 40–60, driven by the northern polar region and possibly connected to the higher climate sensitivity.

The two idealised ACCESS-CM2 runs (*abrupt-4xCO2* and *1pctCO2*) reach very similar levels of minimum sea ice, compared to the two idealised ACCESS-ESM1.5 runs where the *1pctCO2* sea-ice area does not drop as low as in the *abrupt-4xCO2*. This is likely due to the late-simulation increase in surface temperature in the ACCESS-CM2 *1pctCO2* run, which outstrips the ACCESS-ESM1.5 *1pctCO2* temperature increase after 80 years (see Fig. 1a), likely a result of its higher ECS. Total ocean temperature (Fig. 1d) increases more slowly than the surface air temperature, particularly in the *abrupt-4xCO2* simulation, reflecting the time taken for heat to be transported into the deep ocean.

As described in Pincus *et al.* (2016), a series of atmosphere-only experiments have been performed, as part of RFMIP, to characterise the ERF due to human and natural forcings to the climate. Thirty-year simulations were performed using climatologies of sea surface temperature and sea ice taken from the *piControl* run and forced with one of the following: pre-industrial conditions (*piClim-control*), all present-day anthropogenic forcing (*piClim-anthro*), present-day GHG concentrations (*piClim-ghg*), present-day aerosols (*piClim-aer*), present-day land-use forcing separately (*piClim-lu*; ACCESS-ESM1.5 only) or quadrupled CO<sub>2</sub> (*piClim-4xCO2*; which is subsequently scaled by a factor of 0.2266 to be equivalent to the present-day CO<sub>2</sub> concentration of  $1.4 \times$  pre-industrial CO<sub>2</sub>, and is used to separate out the forcing from CO<sub>2</sub> from other greenhouse gases). The ERF values from

**Table 7.** Effective radiative forcing from RFMIP experiments ( $\text{W m}^{-2}$ ).

ERF	ACCESS-CM2	ACCESS-ESM1.5	HadGEM3-GC31-LL	CMIP6
piClim-control	0.24	-0.02		
piClim-4xCO2	7.95	7.04	8.09	$7.98 \pm 0.38$
scaled-1.4xCO2	1.80	1.60	1.83	$1.81 \pm 0.09$
piClim-ghg	3.04	3.06	3.11	$2.89 \pm 0.19$
piClim-aer	-1.09	-1.14	-1.10	$-1.01 \pm 0.23$
piClim-anthro	1.90	2.12	1.81	$2.00 \pm 0.23$
piClim-lu	-	0.05	-0.11	$-0.09 \pm 0.13$

All values other than for *piClim-control* are scaled according to *piClim-control*; including those of HadGEM3-GC31-LL and CMIP6, the values for which are sourced from Smith et al. (2020).

these experiments, and the scaled 1.4xCO<sub>2</sub> value, are presented in Table 7. ACCESS-CM2 simulated a significantly higher 4xCO<sub>2</sub> ERF than ACCESS-ESM1.5, and very close to the CMIP6 mean of  $7.98 \pm 0.38 \text{ W m}^{-2}$  (Smith et al. 2020). This is mostly due to an improvement in the representation of CO<sub>2</sub> absorption in the band 8–13  $\mu\text{m}$ , which was implemented in GA7.0 and adopted into ACCESS-CM2 (Walters et al. 2019); this is also likely a contributing factor to the high ECS of ACCESS-CM2. ACCESS-ESM1.5 simulated a 4xCO<sub>2</sub> ERF of  $7.04 \text{ W m}^{-2}$ , similar to that of the CMIP5 models HadGEM2-ES ( $6.99 \text{ W m}^{-2}$ , which uses a similar atmosphere; Andrews et al. 2012) and ACCESS1.3 ( $6.75 \text{ W m}^{-2}$ , the predecessor of ACCESS-ESM1.5). The GHG, aerosol, anthropogenic and land-use (ACCESS-ESM1.5 only) ERF values for both ACCESS models are similar to those of HadGEM3-GC31-LL, and sit well within the spread of CMIP6 values (Smith et al. 2020).

ACCESS-ESM1.5 has been used to run experiments for C4MIP (including ZECMIP) and CDRMIP that are variants of the *1pctCO2* simulation, or branch from the *1pctCO2* simulation; many of these utilise the interactive carbon cycle. Global average surface CO<sub>2</sub> concentration for emissions-driven experiments are shown in Fig. 2 and global mean *tas* for all C4MIP and CDRMIP experiments is shown in Fig. 3. The response of the carbon cycle is discussed in Section 2.3. For climate–carbon feedback analysis, *1pctCO2* simulations are performed where only the radiation scheme (*1pctCO2-rad*) or only the biogeochemistry (*1pctCO2-bgc*) is subject to increasing atmospheric CO<sub>2</sub>. As expected, *tas* increases in the *1pctCO2-rad* experiment (only slightly less than in *1pctCO2*) whereas the *1pctCO2-bgc* simulation shows only a very small temperature increase. The small differences in temperature response between *1pctCO2-rad* and *1pctCO2* and between *1pctCO2-bgc* and *piControl* are due to feedbacks between the carbon cycle and climate, principally through changes in the evolution of leaf area index and surface albedo. The ACCESS-ESM1.5 temperature response is in the middle of the range of CMIP6 models (Arora et al. 2020).

The C4MIP-ZECMIP experiments (Jones et al. 2019) explore the response of the climate to an abrupt shift to

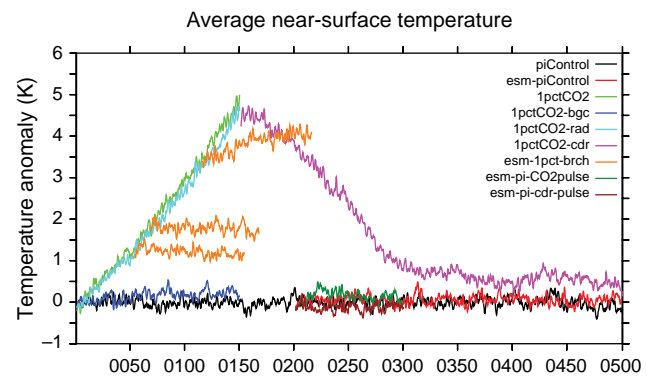


**Fig. 3.** Trends in anomalies of average global surface temperature from extra idealised experiments with ACCESS-ESM1.5. For clarity, emission driven experiments (*esm-piControl*, *esm-pi-CO2pulse* and *esm-pi-cdr-pulse*) start at year 0201 rather than 0001. 12-month boxcar filters have been applied to all metrics.

zero CO<sub>2</sub> emissions. Simulations start at various points from *1pctCO2*, a prescribed concentration experiment, and continue as emissions-driven experiments (with zero emissions). The temperature response is small in all cases, with a slight cooling for the lowest branch, almost no change in temperature for the middle branch and a small warming for the highest branch. Most CMIP6 models show more cooling than ACCESS-ESM1.5 but the spread across models (as given by the standard deviation) is larger than the mean or median cooling (MacDougall et al. 2020).

ACCESS-ESM1.5 has completed three CDRMIP experiments. The reversibility of the climate system is tested in *1pctCO2-cdr* by extending the *1pctCO2* simulation for 140 years with atmospheric CO<sub>2</sub> reducing by 1% per year, and then running for 620 years with pre-industrial CO<sub>2</sub> (noting only 220 years are shown in Fig. 3). With similar results to Ziehn et al. (2020d), in which the previous ACCESS-ESM version was used, global mean *tas* remains  $\sim 1 \text{ K}$  above the pre-industrial temperature at the end of the CO<sub>2</sub> decrease and only slowly decreases over the following centuries, remaining  $0.3 \text{ K}$  above pre-industrial after 600 years.

A further two CDRMIP experiments are perturbations to the *esm-piControl*, and are run in emissions-driven mode. Atmospheric CO<sub>2</sub> is instantaneously increased or decreased by 47 ppm (equivalent to 100 Pg C) to examine the response to the perturbation over 90 years and whether that response is symmetric. The magnitudes of differences in global mean *tas* are small ( $< \pm 0.4$  K, see Fig. 3), with the positive temperature difference (due to the positive CO<sub>2</sub> perturbation) being somewhat larger and shorter lived than the negative temperature difference from the negative CO<sub>2</sub> perturbation. However, another positive temperature difference occurs in the last decade of the simulation due to variability and a decrease in temperature in the *esm-piControl*. This suggests that an ensemble (currently planned) is needed to better constrain the temperature response.

### 3.3. Biogeochemistry in idealised experiments

Global mean ACCESS-ESM1.5 biogeochemical metrics from CMIP6 idealised experiments are shown in Fig. 4 and 5. Fig. 4 includes DECK experiments (*piControl*, *abrupt-4xCO2* and *1pctCO2*) as well as experiments where the atmospheric CO forcing in the *1pctCO2* simulation is applied separately to the radiation or biogeochemical components of the model. Fig. 5 shows experiments that branch from *1pctCO2* (including experiments associated with ZECMIP and CDRMIP) as well as emission-driven experiments (*esm-piControl*, pulse experiments).

Both Fig. 4 and 5 show CO<sub>2</sub> flux and productivity from the land (top rows) and the ocean (middle); ocean O<sub>2</sub> flux and acidification are in the bottom rows. Metrics are filtered by 5- or 1-year box-car filters to remove the seasonal cycle and to reduce large interannual variability, in order to better reveal the differences between simulations.

#### 3.3.1. Land biogeochemistry

The net land carbon flux (Fig. 4a) is the difference between photosynthesis and respiration, and is generally small (in the time mean) except where atmospheric CO<sub>2</sub> is changing. The land net primary productivity (NPP, Fig. 4b) shows carbon uptake by plants (which is approximately balanced by soil respiration). The *abrupt-4xCO2* simulation shows uptake of carbon to the land initially, and a large increase in NPP because photosynthesis responds more quickly to the increased CO<sub>2</sub> than does respiration. Although the net land carbon flux returns close to zero within ~40 years, NPP (Fig. 4b) remains ~18% higher than the control due to the elevated atmospheric CO<sub>2</sub>. This indicates that soil respiration is also elevated relative to the control, given the approximately zero net land flux. Increasing CO<sub>2</sub> in the *1pctCO2* experiment produces increasing NPP through most of the experiment, though the rate of increase declines after ~30 years. This leads to a peak in the net land carbon flux after 20–30 years and then a decline back to around zero mean flux after 100 years. This return to zero land flux is

unusual compared to most other CMIP6 Earth System Models (Arora *et al.* 2020), which tend to produce net land carbon uptake throughout the simulation; the multimodel mean land carbon flux from fig. 2 of Arora *et al.* (2020) is 3.8 Pg C year<sup>-1</sup> at year 0140 (when the *1pctCO2* atmospheric CO<sub>2</sub> reaches four times pre-industrial CO<sub>2</sub>). Across these 140 years, the cumulative land carbon uptake for ACCESS-ESM1.5 (215 Pg C) is lower than other models (408–1204 Pg C); models with nitrogen limitation give lower carbon uptake (mean 536 Pg C) compared with those without (mean 754 Pg C) (Arora *et al.* 2020, fig. 4). ACCESS-ESM1.5 has been run with both nitrogen and phosphorus limitation, and Ziehn *et al.* (2021b) shows that this contributes to the smaller land carbon uptake.

The separate impacts of warming and increased CO<sub>2</sub> on the land carbon fluxes can be seen in the *1pctCO2-rad* and *1pctCO2-bgc* experiments. After an initial rise of 10 Pg C year<sup>-1</sup> over the first 30 years, NPP increases (if slowly) throughout the *1pctCO2-bgc* experiment due to increasing CO<sub>2</sub> but no significant change in temperature (Fig. 3). This is in contrast to the *1pctCO2* run in which NPP declines slightly after approximately 120 years. The impact of warming is confirmed by the *1pctCO2-rad* experiment, where NPP decreases substantially when warming occurs but the carbon cycle does not experience increasing CO<sub>2</sub>. The response in NPP is also reflected in the response of the net land carbon flux. After the initial increase in land carbon uptake, the decrease in net land carbon uptake in the *1pctCO2-bgc* case is slower than in the *1pctCO2* case, remaining ~1 Pg C year<sup>-1</sup> at the end of the simulation. The *1pctCO2-rad* experiment shows an increasing carbon release from the land as expected. While following the general response of other CMIP6 models in these experiments, ACCESS-ESM1.5 experiences less carbon uptake than other models in the *1pctCO2-bgc* experiment, and releases more carbon than almost all models in the *1pctCO2-rad* experiment (Arora *et al.* 2020, fig. A1).

The carbon fluxes for the four experiments that branch from the *1pctCO2* simulation (three ZECMIP and CDRMIP reversibility) are shown in Fig. 5. The ZECMIP experiments show a very small decline in land NPP relative to the *1pctCO2* simulation, but this decline is not seen in the net land flux. Given the relatively small changes in temperature and atmospheric CO<sub>2</sub> simulated in each of these branch experiments (Fig. 2, 3), it is to be expected that a land biosphere approximately in balance (as indicated by the near zero net land flux in *1pctCO2*) would remain in balance and continue to give approximately zero net land flux.

Where the ZECMIP experiments show the response of the carbon fluxes to a relatively slow decrease in atmospheric CO<sub>2</sub>, the CDRMIP reversibility (*1pctCO2-cdr*) experiment shows the response to a relatively large decrease. The net land flux initially remains close to zero, but from around year 0220 becomes increasingly negative, indicating a source of carbon to the atmosphere. The maximum source occurs around year 0280, coincident with atmospheric CO<sub>2</sub>

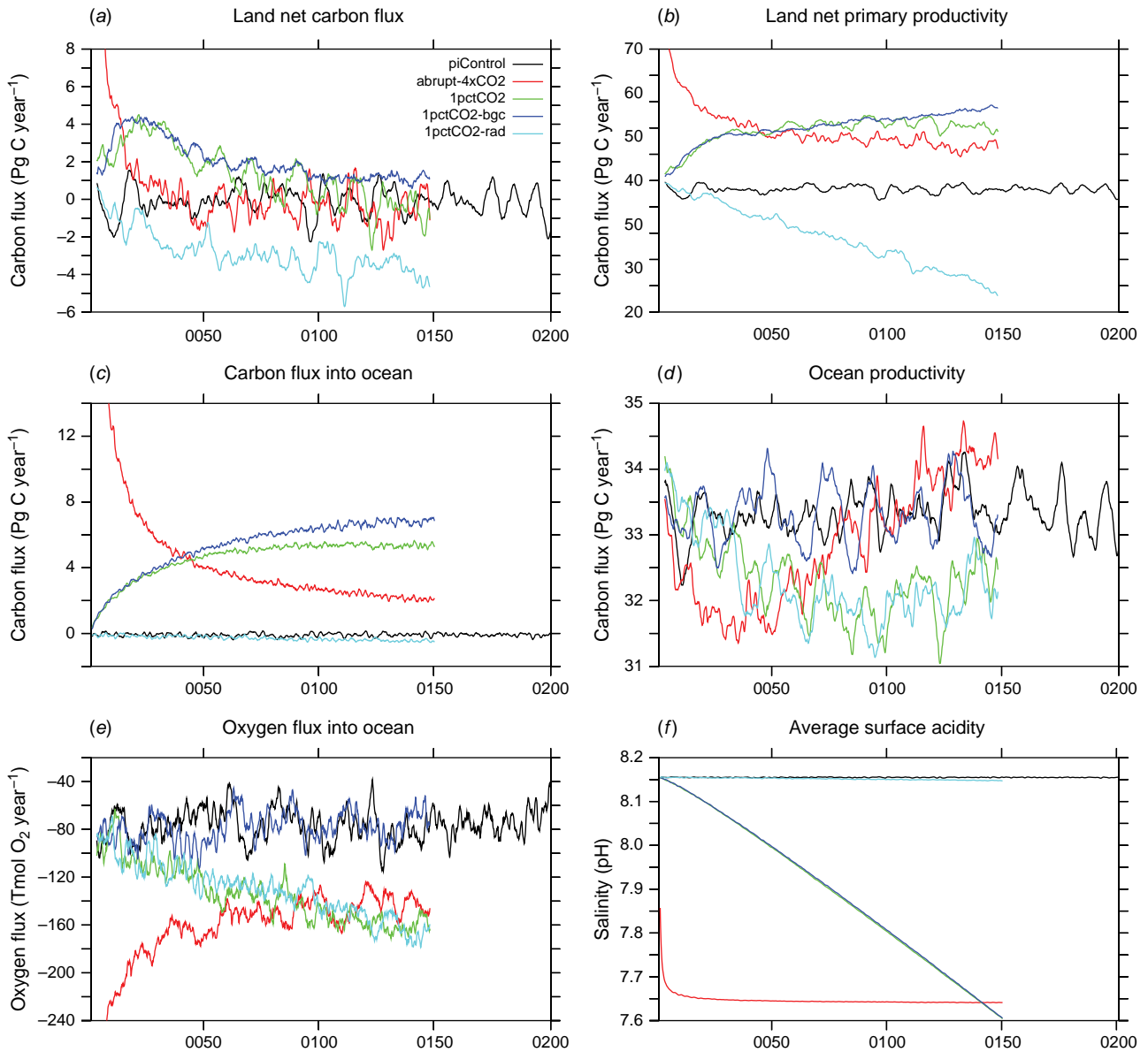


**Fig. 4.** Global biogeochemical metrics from idealised experiments: the *piControl*, *abrupt-4xCO2*, *1pctCO2*, *1pctCO2-bgc* and *1pctCO2-rad*. Trends are shown of carbon flux into the land (top left), net land primary productivity (top right), carbon flux into the ocean (middle left), primary ocean productivity (middle right), oxygen flux into the ocean (bottom left) and average sea surface pH (bottom right) from idealised CMIP experiments with ACCESS-ESM1.5. Sixty-month boxcar filters have been applied to remove seasonal cycles and reduce interannual variability in all metrics, except ocean carbon flux and pH which were filtered with a 12-month boxcar to better reveal the differences between simulations for these variables.

returning to pre-industrial levels, after which the flux returns to approximately zero over  $\sim 30$  years. This behaviour is reflected in the land NPP, which initially decreases slowly, then more rapidly, dropping below the pre-industrial NPP around year 0280, before returning close to, but lower than, pre-industrial NPP. The overshoot and return to pre-industrial land fluxes likely results from the slower return of temperature to pre-industrial compared with atmospheric  $\text{CO}_2$ . The overshoot to below pre-industrial net land carbon flux and NPP is widespread globally but analysis of an

earlier, similar simulation by Ziehn et al. (2020d) showed a variation in response timing at regional scale. Responses varied due to the dominant vegetation type in a region, whether a region was driven more strongly by variations in temperature or precipitation and from the interaction of carbon pools with different turnover times. These regional responses are being further explored in a multimodel study in preparation.

Also shown in Fig. 5 are the BGC responses to the CDRMIP pulse experiments. The abrupt increase or decrease



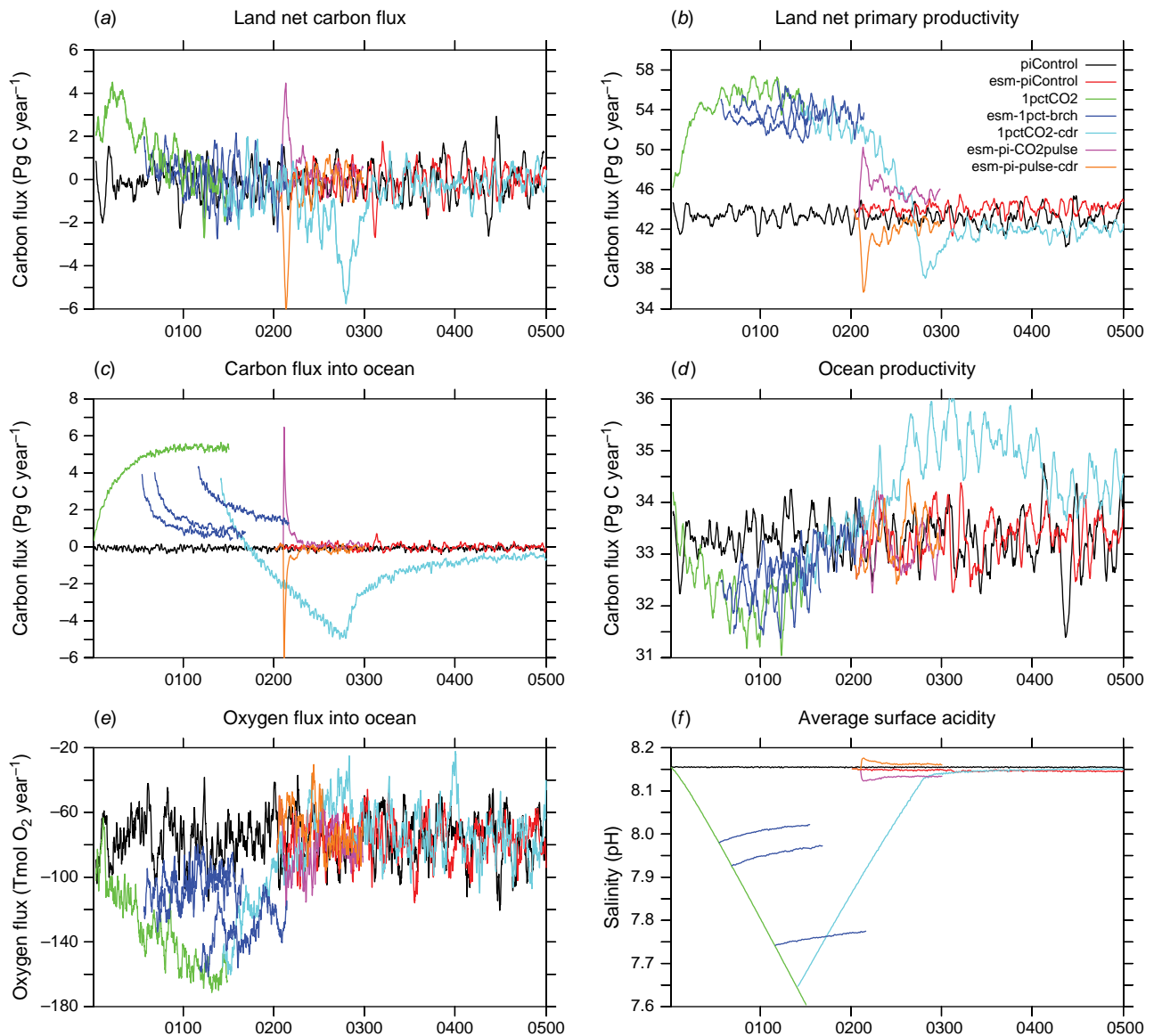


**Fig. 5.** Global biogeochemical metrics from idealised experiments; the *piControl*, *esm-piControl*, *1pctCO2-rev*, zero-emission and pulse experiments, with the same layout as Fig. 4. For clarity, emission driven experiments (*esm-piControl*, pulse and pulse-cdr) start at year 0201 rather than 0001.

in atmospheric  $\text{CO}_2$  (Fig. 2) leads to positive or negative pulses of land  $\text{CO}_2$  fluxes. When  $\text{CO}_2$  is added to the atmosphere, the NPP increases by  $\sim 20\%$ , decreasing to  $\sim 5\%$  above pre-pulse levels by the end of the simulation. The land takes up  $8 \text{ Pg C}$  in the year that the pulse of  $\text{CO}_2$  is put into the atmosphere, but the large uptake is short-lived. When  $\text{CO}_2$  is removed, the decrease in NPP is  $15\text{--}20\%$  over 6 years before increasing to  $\sim 3\%$  below pre-pulse levels. The loss of carbon from the land is  $5\text{--}6 \text{ Pg C}$  for the first 5 years after the negative pulse of atmospheric  $\text{CO}_2$ . Of the  $100 \text{ Pg C}$  added to the atmospheric  $\text{CO}_2$ ,  $\sim 40 \text{ Pg C}$  is taken up by the land with most of the uptake occurring in the first 40 years. When  $100 \text{ Pg C}$  is removed from the atmosphere,

the land loses  $\sim 50 \text{ Pg C}$  over 40 years but then slowly takes up carbon, giving a loss of  $\sim 40 \text{ Pg C}$  by the end of the simulation. The relatively small asymmetry in global land carbon response from the positive and negative  $\text{CO}_2$  pulses should be confirmed regionally, and the analysis of these simulations would benefit from an ensemble of runs, which are currently planned.

### 3.3.2. Ocean biogeochemistry

The latter four panels in Fig. 4 and 5 capture various aspects of the ocean biogeochemistry in the idealised experiments run with ACCESS-ESM1.5. The surface carbon flux

into the ocean (Fig. 4c, 5c) is driven by the difference in CO<sub>2</sub> partial pressure across the ocean–atmosphere surface, and is largely controlled by physical processes and the changing atmospheric CO<sub>2</sub>. Ocean productivity (Fig. 4d, 5d) is mainly constrained by the supply of nutrients into the upper ocean, where solar radiation can drive biological growth. The O<sub>2</sub> flux across the ocean surface (Fig. 4e, 5e) is also related to ocean circulation, as well as temperature. Trends in surface acidity (Fig. 4f, 5f) are dominated by the atmospheric CO<sub>2</sub>, with some influence from the existing alkalinity of the surface ocean. The CO<sub>2</sub> flux and ocean acidification show the least variability, being almost a direct response to atmospheric forcing. Other metrics (e.g. productivity and O<sub>2</sub> flux) are more sensitive to other conditions, such as temperature and ocean dynamics, and are more variable.

The largest carbon fluxes into the ocean are in the *abrupt-4xCO2* experiment, which imposes a high constant atmospheric CO<sub>2</sub> boundary condition and results in a flux into the ocean that reduces after the initial shock. A high CO<sub>2</sub> flux also occurs in the *1pctCO2* experiment, where the increasing atmospheric CO<sub>2</sub> drives an increasing flux over the first few decades. A maximum flux in *1pctCO2* is reached when the value of the Revelle factor increases (e.g. Jiang et al. 2019), reducing the efficiency of CO<sub>2</sub> uptake into the ocean. Mean ocean uptake over the last 30 years of the simulation is 5.3 Pg C year<sup>-1</sup> which is slightly larger than the CMIP6 multimodel mean of 5.0 Pg C year<sup>-1</sup> (Arora et al. 2020, fig. 2).

In experiments that branch from *1pctCO2* (i.e. ZECMIP and *1pctCO2-cdr*), the ocean takes up CO<sub>2</sub> relatively strongly at the branch points (Fig. 5c). In the ZECMIP experiments this uptake decreases after the change to zero emissions, initially rapidly and then more slowly. This is driven by the stabilisation of the atmospheric CO<sub>2</sub> and the reduction in the difference between ocean and atmospheric CO<sub>2</sub> partial pressures. In *1pctCO2-cdr*, the ocean changes from a sink to a source after 30 years because the atmospheric CO<sub>2</sub> drops below the average partial pressure of CO<sub>2</sub> in the surface ocean. The source increases in magnitude until atmospheric CO<sub>2</sub> stabilises at pre-industrial levels, after which the ocean flux slowly returns towards zero.

Also shown in Fig. 5 are the BGC responses to the CDRMIP pulse experiments. The abrupt increase or decrease in atmospheric CO<sub>2</sub> (Fig. 2) leads to positive or negative pulses of ocean carbon fluxes, similar to those seen in the land carbon fluxes. The response is reasonably symmetric for the ocean flux, with the pulse decaying over ~20 years. Of the 100 Pg C added to or removed from the atmosphere, the ocean carbon absorption or release is ~30 Pg C by the end of the run, with 50% of the total absorption or release occurring in the first 5 years.

Average ocean productivity is 33.5 Pg C year<sup>-1</sup> in the *piControl*. Initial reductions in productivity of the order of ~2 Pg C year<sup>-1</sup> are evident in both the *abrupt-4xCO2* and *1pctCO2* experiments (Fig. 4d). Interestingly, these two experiments show an increase in productivity after their

initial decrease and, by the end of the *abrupt-4xCO2* case, global productivity becomes greater than that of the *piControl* experiment. There is considerable uncertainty in the productivity response from high-end climate change scenarios; the standard deviation between CMIP6 models of changes in global ocean productivity in *ssp585* experiments is greater than the multimodel mean (Kwiatkowski et al. 2020). Preliminary analysis shows that ocean productivity changes are not a simple, uniform global response, but rather that local productivity can increase or decrease in different regions driven by regional changes in temperature, mixed layer depth or nutrient supply (not shown in the global analysis).

In *1pctCO2-bgc*, the CO<sub>2</sub> fertilisation experiment, there is negligible impact on productivity and O<sub>2</sub> fluxes compared with *1pctCO2*, whereas in *1pctCO2-rad* productivity and O<sub>2</sub> flux respond in the same way as *1pctCO2*. There is no CO<sub>2</sub> fertilisation process in the ocean biogeochemistry component of the ACCESS-ESM1.5. Hence, productivity in *1pctCO2-bgc* follows the *piControl*, and in *1pctCO2-rad* follows *1pctCO2*.

The O<sub>2</sub> flux trends (Fig. 4e, 5e) respond to changes in ocean circulation, temperature and productivity but, unlike CO<sub>2</sub> fluxes, there is no change in the direct atmospheric forcing for O<sub>2</sub>. There is a non-zero O<sub>2</sub> flux in *piControl* (~-76.4 Tmol O<sub>2</sub> year<sup>-1</sup>) due to the remineralisation of detritus in regions with zero O<sub>2</sub> in the model, as discussed in Ziehn et al. (2020a). In *abrupt-4xCO2*, the balance in the O<sub>2</sub> flux is broken by rapid stratification of the ocean, increasing the vertical stability in the ocean and shutting down the uptake of O<sub>2</sub>. There is an increase in O<sub>2</sub> outgassing in *1pctCO2* and *1pctCO2-rad* as both stratification and surface temperature rise, which is equivalent to the deoxygenation of the ocean in climate change scenarios of ACCESS and other CMIP6 models discussed by Kwiatkowski et al. (2020). The O<sub>2</sub> outgassing reduces in all experiments branching from *1pctCO2* (Fig. 5e). In *1pctCO2-cdr*, O<sub>2</sub> flux reaches parity with *piControl* after ~100 years, followed by a relative influx for ~50 years until atmospheric CO<sub>2</sub> is reduced to pre-industrial levels. This late influx of O<sub>2</sub> is small relative to the outgassing, such that the total ocean O<sub>2</sub> content is reduced by ~5% relative to the pre-industrial content.

Ocean acidity is not a direct model output of ACCESS-ESM1.5, but can be diagnosed from other ocean carbon variables; the metric previously has been used in model intercomparisons of stresses on marine ecosystems (e.g. Bopp et al. 2013; Kwiatkowski et al. 2020). Acidity is calculated from dissolved inorganic carbon, alkalinity and equilibrium solubility constants. These constants are functions of temperature and salinity, and are determined with the same subroutines used to calculate air–sea CO<sub>2</sub> fluxes within the ocean model. Trends in surface ocean acidity (Fig. 4f, 5f) closely follow the atmospheric CO<sub>2</sub> boundary condition (Fig. 2), with minimal variability. Notable from the trends

shown, and particularly for the branching experiments (ZECMIP and CDRMIP-pulse experiments), is that ocean acidification and atmospheric CO<sub>2</sub> are slow to recover from their perturbed states, certainly beyond the 100-year span of the experiments shown. Trends in surface alkalinity due to changes in ocean structure and circulation have a small influence on average acidity as seen in the difference between *1pctCO2-rad* and *piControl*, and that acidity in *1pctCO2-cdr* does not return to pre-industrial values.

## 4. Conclusions

The CMIP6 submission of ACCESS simulation data is much more extensive than the CMIP5 submission, which utilised the models ACCESS1.0 and ACCESS1.3 (Dix *et al.* 2013). A number of factors contributed to this increase, including the greater scope of CMIP6, the additional capability of the models (ACCESS-ESM1.5 is the first Australian submission with carbon cycle capability), and sufficient compute and data storage resources at the modelling group's disposal. Compute resources were larger than originally planned due to the awarding of an Australasian Leadership Computing Grant, which enabled DAMIP simulations and an increase in ensemble size for *historical* and ScenarioMIP experiments. The CMIP6 submission is a major achievement for a relatively small core team especially since the models used for CMIP6 differed more from each other than the two model versions used for CMIP5 and hence had different requirements for their experimental set-up. The OMIP submission would not have been achieved without the COSIMA contribution.

While the ACCESS-ESM1.5 submission was primarily undertaken for the purpose of including Earth system components, the different atmospheric configuration and consequently lower climate sensitivity (compared to ACCESS-CM2) provides good opportunities for comparative studies of the climate generated by each version. The lower compute resource requirement for ACCESS-ESM1.5 has also facilitated additional model use, such as the university-led palaeoclimate simulations contributed to PMIP (Yeung *et al.* 2021; Choudhury *et al.* 2022).

It is difficult to fully track the uptake and use of CMIP6 datasets. The Earth System Grid Federation provides statistics of dataset publications and downloads,<sup>20</sup> noting that in this context each variable for each experiment is counted as a separate dataset, with further versions also counting as additional datasets. These statistics show that there have been over 51 million downloads of the ACCESS datasets

(accessed 11 April 2022) since the first datasets were submitted in December 2019. These download numbers are comparable to models from major international modelling groups, with ACCESS-ESM1.5 in the top 10 models using this download metric.

The number of publications using ACCESS CMIP6 datasets is increasing. The ACCESS-CM2 AMIP simulations are the basis of a paper by Bodman *et al.* (2020), and an evaluation of historical climate variability and change, as simulated by the ACCESS models, is presented in Rashid *et al.* (2022). Ziehn *et al.* (2021b) explores land carbon-concentration and carbon-climate feedbacks using ACCESS-ESM1.5 simulations, whereas Holmes *et al.* (2022) provides an analysis of ocean warming in ACCESS-CM2. ACCESS data have also been used in many multimodel analyses (e.g. Watterson *et al.* 2021; Huang *et al.* 2022). CMIP6 publications are tracked at the CMIP Publication Hub,<sup>21</sup> which lists 208 publications (as of 8 April 2022), though tracking is dependent on authors adding their publication details, optionally with the models that have been included in their analysis. The number of publications that list the inclusion of ACCESS-CM2 or ACCESS-ESM1.5 is comparable to the number listed for other well-respected models. Papers that have used ACCESS-OM2 code or data are also tracked independently,<sup>22</sup> indicating 35 such publications.

ACCESS-CMIP6 data are also now being used as forcing inputs for regional downscaling activities, including CORDEX-CMIP6<sup>23</sup> (Gutowski *et al.* 2016), COWCLIP<sup>24</sup> and Australian national and state climate projections (e.g. Di Virgilio *et al.* 2022). Further use of the ACCESS models and their CMIP6 datasets is welcomed, with information on the availability of ACCESS software and data provided in the next section.

## 5. Code and data availability

Owing to licensing restrictions, we cannot provide either the source code or documentation papers for the UM, which is used under a license and collaborative partnership. For information on obtaining a license for the UM go to <http://www.metoffice.gov.uk/research/collaboration/um-collaboration>. CABLE is distributed under an open source license. It is hosted at NCI, and registration is required to access the code repository. Details can be found at [https://trac.nci.org.au/trac/cable/wiki/CABLE\\_Registration](https://trac.nci.org.au/trac/cable/wiki/CABLE_Registration). MOM5 is available to download from <https://github.com/mom-ocean/MOM5> (ACCESS-CM2) and <https://github.com/COSIMA/ACCESS-ESM1.5-MOM5> (ACCESS-ESM1.5, with WOMBAT). CICE is available at <https://github.com/COSIMA/cice5>

<sup>20</sup><http://esgf-ui.cmcc.it/esgf-dashboard-ui/cmip6.html>

<sup>21</sup><https://cmip-publications.llnl.gov>

<sup>22</sup>[https://scholar.google.com/citations?hl=en&user=inVqu\\_4AAAAJ](https://scholar.google.com/citations?hl=en&user=inVqu_4AAAAJ)

<sup>23</sup><https://cordex.org/>

<sup>24</sup><https://cowclip.org/>

(ACCESS-CM2, ACCESS-OM2) and <https://github.com/COSIMA/cice4> (ACCESS-ESM1.5). The OASIS3-MCT coupler is available at <https://github.com/COSIMA/oasis3-mct>. ACCESS-OM2 code is available at <https://github.com/COSIMA/access-om2> and the version at the time of OMIP submission is available at <https://github.com/COSIMA/access-om2/releases/tag/2020-11-12>. The ACCESS-OM2 configurations used for CMIP6 submission include the following: [https://github.com/COSIMA/1deg\\_jra55\\_iaf/tree/omip2](https://github.com/COSIMA/1deg_jra55_iaf/tree/omip2) and [https://github.com/COSIMA/1deg\\_jra55\\_iaf/tree/omip2spunup](https://github.com/COSIMA/1deg_jra55_iaf/tree/omip2spunup) for ACCESS-OM2; and [https://github.com/COSIMA/025deg\\_jra55\\_iaf/tree/omip\\_amoctopo\\_cycle1](https://github.com/COSIMA/025deg_jra55_iaf/tree/omip_amoctopo_cycle1) through to [https://github.com/COSIMA/025deg\\_jra55\\_iaf/tree/omip\\_amoctopo\\_cycle6](https://github.com/COSIMA/025deg_jra55_iaf/tree/omip_amoctopo_cycle6) for ACCESS-OM2-025. Rose/cycl suits, which each contain the experiment configuration of a single ACCESS-CM2 realisation, are held in a revision-controlled repository service hosted at the UKMO. A mapping between suite names and CMIP6 ensemble members can be found at <https://confluence.csiro.au/display/ACCESS/CMIP6+Archive+-+ACCESS-CM2>. *Payu* configurations for the ACCESS-ESM1.5 experiments *piControl*, *historical* and *PMIP* can be found at the CLEX GitHub repository <https://github.com/coecms> (e.g. <https://github.com/coecms/esm-lig>). Configurations for ACCESS-OM2 can be found at the COSIMA GitHub repository <https://github.com/COSIMA>. The APP4 post-processing code used to CMORise ACCESS model output is available at <https://git.nci.org.au/cm2704/APP4> (Mackallah et al. 2022). The mapping between ACCESS output fields and CMIP6 variables is specified in the file *APP4/input\_files/master\_map\_om2.csv*. Both *python2* and *cdms2* will soon be no longer supported, therefore reproducibility is enabled and ensured through a Conda environment. Future development and access to this tools will be facilitated by the ACCESS-NRI.<sup>25</sup> CMORised simulation data are published on the Earth System Grid at Dix et al. (2019a) (ACCESS-CM2), Ziehn et al. (2019c) (ACCESS-ESM1.5), Hayashida et al. (2021) (ACCESS-OM2) and Holmes et al. (2021) (ACCESS-OM2-025). See also <https://esgf.nci.org.au/search/cmip6-nci> (ESGF data portal, NCI node) and <https://doi.org/10.25914/5e6acd0492b39> (NCI GeoNetwork record). NCI users can also access the data directly from project fs38 (<https://my.nci.org.au/mancini/project/fs38>). Model output, the semi-processed simulation data which include many variables not requested by CMIP6, that has not been CMORised is also available for NCI users in project p73 (<https://my.nci.org.au/mancini/project/p73>).

## References

Andrews T, Gregory JM, Webb MJ, Taylor KE (2012) Forcing, feedbacks and climate sensitivity in CMIP5 coupled atmosphere–ocean climate models. *Geophysical Research Letters* **39**, L09712. doi:10.1029/2012GL051607

Arfeuille F, Weisenstein D, Mack H, Rozanov E, Peter T, Brönnimann S (2014) Volcanic forcing for climate modeling: a new microphysics-based

data set covering years 1600–present. *Climate of the Past* **10**, 359–375. doi:10.5194/cp-10-359-2014

Arora VK, Katavouta A, Williams RG, Jones CD, Brovkin V, Friedlingstein P, Schwinger J, Bopp L, Boucher O, Cadule P, Chamberlain MA, Christian JR, Delire C, Fisher RA, Hajima T, Ilyina T, Joetzjer E, Kawamiya M, Koven CD, Krasting JP, Law RM, Lawrence DM, Lenton A, Lindsay K, Pongratz J, Raddatz T, Séférian R, Tachiiri K, Tjiputra JF, Wiltshire A, Wu T, Ziehn T (2020) Carbon-concentration and carbon–climate feedbacks in CMIP6 models and their comparison to CMIP5 models. *Biogeosciences* **17**, 4173–4222. doi:10.5194/bg-17-4173-2020

Balaji V, Maisonnave E, Zadeh N, Lawrence BN, Biercamp J, Fladrich U, Aloisio G, Benson R, Caubel A, Durachta J, Foujols M-A, Lister G, Mocavero S, Underwood S, Wright G (2017) CPMIP: measurements of real computational performance of Earth system models in CMIP6. *Geoscientific Model Development* **10**, 19–34. doi:10.5194/gmd-10-19-2017

Balaji V, Taylor KE, Jukes M, Lawrence BN, Durack PJ, Lautenschlager M, Blanton C, Cinquini L, Denvil S, Elkington M, Guglielmo F, Guilyardi E, Hassell D, Khari S, Kindermann S, Nikonov S, Radhakrishnan A, Stockhouse M, Weigel T, Williams D (2018) Requirements for a global data infrastructure in support of CMIP6. *Geoscientific Model Development* **11**, 3659–3680. doi:10.5194/gmd-11-3659-2018

Bellouni N, Collins W, Culverwell I, Halloran P, Hardiman S, Hinton T, Jones C, McDonald R, McLaren A, O'Connor F, et al. (2011a) The HadGEM2 family of met office unified model climate configurations. *Geoscientific Model Development* **4**, 723.

Bellouni N, Rae J, Jones A, Johnson C, Haywood J, Boucher O (2011b) Aerosol forcing in the Climate Model Intercomparison Project (CMIP5) simulations by HadGEM2-ES and the role of ammonium nitrate. *Journal of Geophysical Research: Atmospheres* **116**, D20206. doi:10.1029/2011JD016074

Berger A, Loutre MF (1991) Insolation values for the climate of the last 10 million years. *Quaternary Science Reviews* **10**, 297–317. doi:10.1016/0277-3791(91)90033-Q

Best MJ, Pryor M, Clark DB, Rooney GG, Essery RLH, Ménard CB, Edwards JM, Hendry MA, Porson A, Gedney N, et al. (2011) The Joint UK Land Environment Simulator (JULES), model description – part 1: energy and water fluxes. *Geoscientific Model Development* **4**, 677–699. doi:10.5194/gmd-4-677-2011

Bi D, Dix M, Marsland SJ, O'Farrell S, Rashid HA, Uotila P, Hirst AC, Kowalczyk E, Golebiewski M, Sullivan A, Yan H, Hannah N, Franklin C, Sun Z, Vohralik P, Watterson I, Zhou X, Fiedler R, Collier M, Ma Y, Noonan J, Stevens L, Uhe P, Zhu H, Griffies SM, Hill R, Harris C, Puri K (2013) The ACCESS coupled model: description, control climate and evaluation. *Australian Meteorological and Oceanographic Journal* **63**, 41–64. doi:10.22499/2.6301.004

Bi D, Dix M, Marsland S, O'Farrell S, Sullivan A, Bodman R, Law R, Harman I, Srbinovsky J, Rashid HA, Dobrohotoff P, Mackallah C, Yan H, Hirst A, Savita A, Dias FB, Woodhouse M, Fiedler R, Heerdegen A (2020) Configuration and spin-up of ACCESS-CM2, the new generation Australian Community Climate and Earth System Simulator Coupled Model. *Journal of Southern Hemisphere Earth Systems Science* **70**, 225–251. doi:10.1071/ES19040

Bodman RW, Karoly DJ, Dix MR, Harman IN, Srbinovsky J, Dobrohotoff PB, Mackallah C (2020) Evaluation of CMIP6 AMIP climate simulations with the ACCESS-AM2 model. *Journal of Southern Hemisphere Earth Systems Science* **70**, 166–179. doi:10.1071/ES19033

Bopp L, Resplandy L, Orr JC, Doney SC, Dunne JP, Gehlen M, Halloran P, Heinze C, Ilyina T, Séférian R, Tjiputra J, Vichi M (2013) Multiple stressors of ocean ecosystems in the 21st century: projections with CMIP5 models. *Biogeosciences* **10**, 6225–6245. doi:10.5194/bg-10-6225-2013

Checa-García R, Hegglin MI, Kinnison D, Plummer DA, Shine KP (2018) Historical tropospheric and stratospheric ozone radiative forcing using the CMIP6 database. *Geophysical Research Letters* **45**, 3264–3273. doi:10.1002/grl.v45.7

Choudhury D, Menviel L, Meissner KJ, Yeung NKH, Chamberlain M, Ziehn T (2022) Marine carbon cycle response to a warmer Southern

<sup>25</sup><https://www.access-nri.org.au/>

- Ocean: the case of the last interglacial. *Climate of the Past* **18**, 507–523. doi:10.5194/cp-18-507-2022
- Clark DB, Mercado LM, Sitch S, Jones CD, Gedney N, Best MJ, Pryor M, Rooney GG, Essery RLH, Blyth E, *et al.* (2011) The Joint UK Land Environment Simulator (JULES), model description – part 2: carbon fluxes and vegetation dynamics. *Geoscientific Model Development* **4**, 701–722. doi:10.5194/gmd-4-701-2011
- Collier M, Uhe P (2012) CMIP5 datasets from the ACCESS1.0 and ACCESS1.3 coupled climate models. CAWCR Technical Report Number 059. Available at [https://www.cawcr.gov.au/technical-reports/CTR\\_059.pdf](https://www.cawcr.gov.au/technical-reports/CTR_059.pdf)
- Deser C, Lehner F, Rodgers KB, Ault T, Delworth TL, DiNezio PN, Fiore A, Frankignoul C, Fyfe JC, Horton DE, *et al.* (2020) Insights from Earth system model initial-condition large ensembles and future prospects. *Nature Climate Change* **10**, 277–286. doi:10.1038/s41558-020-0731-2
- Di Virgilio G, Ji F, Tam E, Nishant N, Evans JP, Thomas C, Riley ML, Beyer K, Grose MR, Narsey S, Delage F (2022) Selecting CMIP6 GCMs for CORDEX dynamical downscaling: model performance, independence, and climate change signals. *Earth's Future* **10**, e2021EF002625. doi:10.1029/2021EF002625
- Dix M, Vohralik P, Bi D, Rashid H, Marsland S, O'Farrell S, Uotila P, Hirst T, Kowalczyk E, Sullivan A, Yan H, Franklin C, Sun Z, Watterson I, Collier M, Noonan J, Rotstayn L, Stevens L, Uhe P, Puri K (2013) The ACCESS coupled model: documentation of core CMIP5 simulations and initial results. *Australian Meteorological and Oceanographic Journal* **63**, 83–99. doi:10.22499/2.6301.006
- Dix M, Bi D, Dobrohotoff P, Fiedler R, Harman I, Law R, Mackallah C, Marsland S, O'Farrell S, Rashid H, Srbinovsky J, Sullivan A, Trenham C, Vohralik P, Watterson I, Williams G, Woodhouse M, Bodman R, Dias FB, Domingues C, Hannah N, Heerdegen A, Savita A, Wales S, Allen C, Druken K, Evans B, Richards C, Ridzwan SM, Roberts D, Smillie J, Snow K, Ward M, Yang R (2019a) CSIRO-ARCCSS ACCESS-CM2 model output prepared for CMIP6 CMIP. doi:10.22033/ESGF/CMIP6.2281
- Dix M, Bi D, Dobrohotoff P, Fiedler R, Harman I, Law R, Mackallah C, Marsland S, O'Farrell S, Rashid H, Srbinovsky J, Sullivan A, Trenham C, Vohralik P, Watterson I, Williams G, Woodhouse M, Bodman R, Dias FB, Domingues C, Hannah N, Heerdegen A, Savita A, Wales S, Allen C, Druken K, Evans B, Richards C, Ridzwan SM, Roberts D, Smillie J, Snow K, Ward M, Yang R (2019b) CSIRO-ARCCSS ACCESS-CM2 model output prepared for CMIP6 ScenarioMIP. doi:10.22033/ESGF/CMIP6.2285
- Dix M, Mackallah C, Bi D, Bodman R, Marsland S, Rashid H, Woodhouse M, Druken K (2020a) CSIRO-ARCCSS ACCESS-CM2 model output prepared for CMIP6 DAMIP. Available at <http://cera-www.dkrz.de/WDC/CMIP6/CMIP6.DAMIP.CSIRO-ARCCSS.ACCESS-CM2>
- Dix M, Mackallah C, Bi D, Bodman R, Marsland S, Rashid H, Woodhouse M, Druken K (2020b) CSIRO-ARCCSS ACCESS-CM2 model output prepared for CMIP6 RFMIP. doi:10.22033/ESGF/CMIP6.2284
- Durack PJ, Taylor KE (2017) PCMDI AMIP SST and sea-ice boundary conditions version 1.1.3. doi:10.22033/ESGF/input4MIPs.1735
- Durack P, Taylor K, Eyring V, Ames S, Hoang T, Nadeau D, Doutriaux C, Stockhouse M, Gleckler P (2018) Toward standardized data sets for climate model experimentation. *Eos* **99**. doi:10.1029/2018EO101751
- Eyring V, Bony S, Meehl GA, Senior CA, Stevens B, Stouffer RJ, Taylor KE (2016) Overview of the Coupled Model Intercomparison Project Phase 6 (CMIP6) experimental design and organization. *Geoscientific Model Development* **9**, 1937–1958. doi:10.5194/gmd-9-1937-2016
- Gillett NP, Shiogama H, Funke B, Hegerl G, Knutti R, Matthes K, Santer BD, Stone D, Tebaldi C (2016) The Detection and Attribution Model Intercomparison Project (DAMIP v1.0) contribution to CMIP6. *Geoscientific Model Development* **9**, 3685–3697. doi:10.5194/gmd-9-3685-2016
- Gregory JM, Ingram WJ, Palmer MA, Jones GS, Stott PA, Thorpe RB, Lowe JA, Johns TC, Williams KD (2004) A new method for diagnosing radiative forcing and climate sensitivity. *Geophysical Research Letters* **31**, L03205. doi:10.1029/2003GL018747
- Gregory JM, Bouttes N, Griffies SM, Haak H, Hurlin WJ, Jungclaus J, Kelley M, Lee WG, Marshall J, Romanou A, Saenko OA, Stammer D, Winton M (2016) The Flux-Anomaly-Forced Model Intercomparison Project (FAFMIP) contribution to CMIP6: investigation of sea-level and ocean climate change in response to CO<sub>2</sub> forcing. *Geoscientific Model Development* **9**, 3993–4017. doi:10.5194/gmd-9-3993-2016
- Griffies SM (2012) Elements of the Modular Ocean Model (MOM), GFDL Ocean Group Technical Report Number 7. (NOAA/Geophysical Fluid Dynamics Laboratory)
- Griffies SM, Danabasoglu G, Durack PJ, Adcroft AJ, Balaji V, Böning CW, Chassignet EP, Curchitser E, Deshayes J, Drange H, Fox-Kemper B, Gleckler PJ, Gregory JM, Haak H, Hallberg RW, Heimbach P, Hewitt HT, Holland DM, Ilyina T, Jungclaus JH, Komuro Y, Krasting JP, Large WG, Marsland SJ, Masina S, McDougall TJ, Nurser AJG, Orr JC, Pirani A, Qiao F, Stouffer RJ, Taylor KE, Treguer AM, Tsujino H, Uotila P, Valdivieso M, Wang Q, Winton M, Yeager SG (2016) OMIP contribution to CMIP6: experimental and diagnostic protocol for the physical component of the Ocean Model Intercomparison Project. *Geoscientific Model Development* **9**, 3231–3296. doi:10.5194/gmd-9-3231-2016
- Grose MR, Narsey S, Delage FP, Dowdy AJ, Bador M, Boschat G, Chung C, Kajtar JB, Rauniyar S, Freund MB, Lyu K, Rashid H, Zhang X, Wales S, Trenham C, Holbrook NJ, Cowan T, Alexander L, Arblaster JM, Power S (2020) Insights from CMIP6 for Australia's future climate. *Earth's Future* **8**, e2019EF001469. doi:10.1029/2019EF001469
- Gutowski WJ Jr, Giorgi F, Timbal B, Frigon A, Jacob D, Kang H-S, Raghavan K, Lee B, Lennard C, Nikulin G, O'Rourke E, Rixen M, Solman S, Stephenson T, Tangang F (2016) WCRP Coordinated Regional Downscaling Experiment (CORDEX): a diagnostic MIP for CMIP6. *Geoscientific Model Development* **9**, 4087–4095. doi:10.5194/gmd-9-4087-2016
- Hardiman SC, Andrews MB, Andrews T, Bushell AC, Dunstone NJ, Dyson H, Jones GS, Knight JR, Neinger E, O'Connor FM, Ridley JK, Ringer MA, Scaife AA, Senior CA, Wood RA (2019) The impact of prescribed ozone in climate projections run with HadGEM3-GC3.1. *Journal of Advances in Modeling Earth Systems* **11**, 3443–3453. doi:10.1029/2019MS001714
- Hayashida H, Kiss A, Hogg A, Hannah N, Dias FB, Brassington G, Chamberlain M, Chapman C, Dobrohotoff P, Domingues C, Duran E, England M, Fiedler R, Griffies SM, Heerdegen A, Heil P, Holmes R, Klocker A, Marsland S, Morrison A, Munroe J, Nikurashin M, Oke PR, Pilo GS, Richet O, Savita A, Spence P, Stewart KD, Ward M, Wu F, Zhang X, Mackallah C, Druken K (2021) CSIRO-COSIMA ACCESS-OM2 model output prepared for CMIP6 OMIP. doi:10.22033/ESGF/CMIP6.14661
- Hoesly RM, Smith SJ, Feng L, Klimont Z, Janssens-Maenhout G, Pitkanen T, Seibert JJ, Vu L, Andres RJ, Bolt RM, Bond TC, Dawidowski L, Kholod N, Kurokawa J-i, Li M, Liu L, Lu Z, Moura MCP, O'Rourke PR, Zhang Q (2018) Historical (1750–2014) anthropogenic emissions of reactive gases and aerosols from the Community Emissions Data System (CEDS). *Geoscientific Model Development* **11**, 369–408. doi:10.5194/gmd-11-369-2018
- Holmes R, Kiss A, Hogg A, Hannah N, Dias FB, Brassington G, Chamberlain M, Chapman C, Dobrohotoff P, Domingues C, Duran E, England M, Fiedler R, Griffies SM, Heerdegen A, Heil P, Klocker A, Marsland S, Morrison A, Munroe J, Nikurashin M, Oke PR, Pilo GS, Richet O, Savita A, Spence P, Stewart KD, Ward M, Wu F, Zhang X, Mackallah C, Druken K (2021) CSIRO-COSIMA ACCESS-OM2-025 model output prepared for CMIP6 OMIP. doi:10.22033/ESGF/CMIP6.14663
- Holmes RM, Sohail T, Zika JD (2022) Adiabatic and diabatic signatures of ocean temperature variability. *Journal of Climate* **35**, 1459–1477. doi:10.1175/JCLI-D-21-0695.1
- Huang Y, Wang Y-P, Ziehn T (2022) Nonlinear interactions of land carbon cycle feedbacks in Earth System Models. *Global Change Biology* **28**, 296–306. doi:10.1111/gcb.15953
- Hunke EC, Lipscomb WH (2010) 'CICE: The Los Alamos sea ice model documentation and software user's manual, Version 4.1, LA-CC-06-012.' (Los Alamos National Laboratory: Los Alamos, NM, USA)
- Hurt G, Chini L, Sahajpal R, Frolking S, Bodirsky BL, Calvin K, Doelman J, Fisk J, Fujimori S, Goldewijk KK, Hasegawa T, Havlik P, Heinemann A, Humpenöder F, Jungclaus J, Kaplan J, Krisztin T, Lawrence D, Lawrence P, Mertz O, Pongratz J, Popp A, Riahi K, Shevliakova E, Stehfest E, Thornton P, van Vuuren D, Zhang X (2017) Harmonization of global land use scenarios (LUH2): Historical v2.1h 850 - 2015. doi:10.22033/ESGF/input4MIPs.1127
- Irving D, Hobbs W, Church J, Zika J (2021) A mass and energy conservation analysis of drift in the CMIP6 ensemble. *Journal of Climate* **34**, 3157–3170. doi:10.1175/JCLI-D-20-0281.1

- Jiang L-Q, Carter BR, Feely RA, Lauvset SK, Olsen A (2019) Surface ocean pH and buffer capacity: past, present and future. *Scientific Reports* 9, 18624. doi:10.1038/s41598-019-55039-4
- Jones CD, Arora V, Friedlingstein P, Bopp L, Brovkin V, Dunne J, Graven H, Hoffman F, Ilyina T, John JG, Jung M, Kawamiya M, Koven C, Pongratz J, Raddatz T, Randerson JT, Zaehle S (2016) C4MIP – the Coupled Climate–Carbon Cycle Model Intercomparison Project: experimental protocol for CMIP6. *Geoscientific Model Development* 9, 2853–2880. doi:10.5194/gmd-9-2853-2016
- Jones CD, Frölicher TL, Koven C, MacDougall AH, Matthews HD, Zickfeld K, Rogelj J, Tokarska KB, Gillett NP, Ilyina T, Meinshausen M, Mengis N, Séférian R, Eby M, Burger FA (2019) The Zero Emissions Commitment Model Intercomparison Project (ZECMIP) contribution to C4MIP: quantifying committed climate changes following zero carbon emissions. *Geoscientific Model Development* 12, 4375–4385. doi:10.5194/gmd-12-4375-2019
- Jones CD, Hickman JE, Rumbold ST, Walton J, Lamboll RD, Skeie RB, Fiedler S, Forster PM, Rogelj J, Abe M, Botzet M, Calvin K, Cassou C, Cole JNS, Davini P, Deushi M, Dix M, Fyfe JC, Gillett NP, Ilyina T, Kawamiya M, Kelley M, Kharin S, Koshiro T, Li H, Mackallah C, Müller WA, Nabat P, van Noije T, Nolan P, Ohgaito R, Olivé D, Oshima N, Parodi J, Reerink TJ, Ren L, Romanou A, Séférian R, Tang Y, Timmreck C, Tjiputra J, Tourigny E, Tsigaridis K, Wang H, Wu M, Wyser K, Yang S, Yang Y, Ziehn T (2021) The climate response to emissions reductions due to COVID-19: initial results from CovidMIP. *Geophysical Research Letters* 48, e2020GL091883. doi:10.1029/2020GL091883
- Juckes M, Taylor KE, Durack PJ, Lawrence B, Mizielinski MS, Pamment A, Peterschmitt J-Y, Rixen M, Sénési S (2020) The CMIP6 Data Request (DREQ, version 01.00.31). *Geoscientific Model Development* 13, 201–224. doi:10.5194/gmd-13-201-2020
- Kageyama M, Braconnot P, Harrison SP, Haywood AM, Jungclaus JH, Otto-Bliessner BL, Peterschmitt J-Y, Abe-Ouchi A, Albani S, Bartlein PJ, Brierey C, Crucifix M, Dolan A, Fernandez-Donado L, Fischer H, Hopcroft PO, Ivanovic RF, Lambert F, Lunt DJ, Mahowald NM, Peltier WR, Phipps SJ, Roche DM, Schmidt GA, Tarasov L, Valdes PJ, Zhang Q, Zhou T (2018) The PMIP4 contribution to CMIP6 – part 1: overview and over-arching analysis plan. *Geoscientific Model Development* 11, 1033–1057. doi:10.5194/gmd-11-1033-2018
- Keller DP, Lenton A, Scott V, Vaughan NE, Bauer N, Ji D, Jones CD, Kravitz B, Muri H, Zickfeld K (2018) The Carbon Dioxide Removal Model Intercomparison Project (CDRMIP): rationale and experimental protocol for CMIP6. *Geoscientific Model Development* 11, 1133–1160. doi:10.5194/gmd-11-1133-2018
- Kiss AE, Hogg AM, Hannah N, Boeira Dias F, Brassington GB, Chamberlain MA, Chapman C, Dobrohotoff P, Domingues CM, Duran ER, England MH, Fiedler R, Griffies SM, Heerdegen A, Heil P, Holmes RM, Klockner A, Marsland SJ, Morrison AK, Munroe J, Nikurashin M, Oke PR, Pilo GS, Richet O, Savita A, Spence P, Stewart KD, Ward ML, Wu F, Zhang X (2020) ACCESS-OM2 v1.0: a global ocean–sea ice model at three resolutions. *Geoscientific Model Development* 13, 401–442. doi:10.5194/gmd-13-401-2020
- Kowalczyk EA, Wang YP, Law RM, Davies HL, McGregor JL, Abramowitz G (2006) The CSIRO Atmosphere Biosphere Land Exchange (CABLE) model for use in climate models and as an offline model. Marine and Atmospheric Research technical paper 13, CSIRO.
- Kowalczyk EA, Stevens L, Law RM, Dix M, Wang YP, Harman IN, Haynes K, Srbinovsky J, Pak B, Ziehn T (2013) The land surface model component of ACCESS: description and impact on the simulated surface climatology. *Australian Meteorological and Oceanographic Journal* 63, 65–82. doi:10.22499/2.6301.005
- Kwiatkowski L, Torres O, Bopp L, Aumont O, Chamberlain M, Christian JR, Dunne JP, Gehlen M, Ilyina T, John JG, Lenton A, Li H, Lovenduski NS, Orr JC, Palmieri J, Santana-Falcón Y, Schwinger J, Séférian R, Stock CA, Tagliabue A, Takano Y, Tjiputra J, Toyama K, Tsjujino H, Watanabe M, Yamamoto A, Yool A, Ziehn T (2020) Twenty-first century ocean warming, acidification, deoxygenation, and upper-ocean nutrient and primary production decline from CMIP6 model projections. *Biogeosciences* 17, 3439–3470. doi:10.5194/bg-17-3439-2020
- Law RM, Ziehn T, Matear RJ, Lenton A, Chamberlain MA, Stevens LE, Wang Y-P, Srbinovsky J, Bi D, Yan H, Vohralik PF (2017) The carbon cycle in the Australian Community Climate and Earth System Simulator (ACCESS-ESM1) – part 1: model description and pre-industrial simulation. *Geoscientific Model Development* 10, 2567–2590. doi:10.5194/gmd-10-2567-2017
- Lawrence DM, Hurtt GC, Arneeth A, Brovkin V, Calvin KV, Jones AD, Jones CD, Lawrence PJ, de Noblet-Ducoudré N, Pongratz J, Seneviratne SI, Shevliakova E (2016) The Land Use Model Intercomparison Project (LUMIP) contribution to CMIP6: rationale and experimental design. *Geoscientific Model Development* 9, 2973–2998. doi:10.5194/gmd-9-2973-2016
- Lee J, Kim J, Sun M-A, Kim B-H, Moon H, Sung HM, Kim J, Byun Y-H (2020) Evaluation of the Korea Meteorological Administration Advanced Community Earth-System model (K-ACE). *Asia-Pacific Journal of Atmospheric Sciences* 56, 381–395. doi:10.1007/s13143-019-00144-7
- MacDougall AH, Frölicher TL, Jones CD, Rogelj J, Matthews HD, Zickfeld K, Arora VK, Barrett NJ, Brovkin V, Burger FA, Eby M, Eliseev AV, Hajima T, Holden PB, Jeltsch-Thömmes A, Koven C, Mengis N, Menviel L, Michou M, Mokhov II, Oka A, Schwinger J, Séférian R, Shaffer G, Sokolov A, Tachiiri K, Tjiputra J, Wiltshire A, Ziehn T (2020) Is there warming in the pipeline? A multi-model analysis of the Zero Emissions Commitment from CO<sub>2</sub>. *Biogeosciences* 17, 2987–3016. doi:10.5194/bg-17-2987-2020
- Mackallah C, Uhe P, Collier M (2022) ACCESS Post-Processor v4. Available at <http://hdl.handle.net/102.100.100/437645?index=1>
- Mann GW, Carslaw KS, Spracklen DV, Ridley DA, Manktelow PT, Chipperfield MP, Pickering SJ, Johnson CE (2010) Description and evaluation of GLOMAP-mode: a modal global aerosol microphysics model for the UKCA composition-climate model. *Geoscientific Model Development* 3, 519–551. doi:10.5194/gmd-3-519-2010
- Matthes K, Funke B, Andersson ME, Barnard L, Beer J, Charbonneau P, Clilverd MA, Dudok de Wit T, Haberreiter M, Hendry A, Jackman CH, Kretzschmar M, Kruschke T, Kunze M, Langematz U, Marsh DR, Maycock AC, Misios S, Rodger CJ, Scaife AA, Seppälä A, Shangguan M, Sinnhuber M, Tourpali K, Usoskin I, van de Kamp M, Verronen PT, Versick S (2017) Solar forcing for CMIP6 (v3.2). *Geoscientific Model Development* 10, 2247–2302. doi:10.5194/gmd-10-2247-2017
- Meehl GA, Senior CA, Eyring V, Flato G, Lamarque J-F, Stouffer RJ, Taylor KE, Schlund M (2020) Context for interpreting equilibrium climate sensitivity and transient climate response from the CMIP6 Earth system models. *Science Advances* 6, eaba1981. doi:10.1126/sciadv.aba1981
- Meinshausen M, Vogel E (2016) input4MIPs.UoM.GHGConcentrations. CMIP.UoM-CMIP-1-2-0. doi:10.22033/ESGF/input4MIPs.1118
- Meinshausen M, Vogel E, Nauels A, Lorbacher K, Meinshausen N, Etheridge DM, Fraser PJ, Montzka SA, Rayner PJ, Trudinger CM, Krummel PB, Beyerle U, Canadell JG, Daniel JS, Enting IG, Law RM, Lunder CR, O'Doherty S, Prinn RG, Reimann S, Rubino M, Velders GJM, Vollmer MK, Wang RHJ, Weiss R (2017) Historical greenhouse gas concentrations for climate modelling (CMIP6). *Geoscientific Model Development* 10, 2057–2116. doi:10.5194/gmd-10-2057-2017
- Meinshausen M, Nicholls ZRJ, Lewis J, Gidden MJ, Vogel E, Freund M, Beyerle U, Gessner C, Nauels A, Bauer N, Canadell JG, Daniel JS, John A, Krummel PB, Luderer G, Meinshausen N, Montzka SA, Rayner PJ, Reimann S, Smith SJ, van den Berg M, Velders GJM, Vollmer MK, Wang RHJ (2020) The shared socio-economic pathway (SSP) greenhouse gas concentrations and their extensions to 2500. *Geoscientific Model Development* 13, 3571–3605. doi:10.5194/gmd-13-3571-2020
- Met Office (2020) Iris: a Python library for analysing and visualising meteorological and oceanographic data sets, Exeter, Devon, v3 edn. Available at <http://scitools.org.uk/>
- Morgenstern O, Hegglin MI, Rozanov E, O'Connor FM, Abraham NL, Akiyoshi H, Archibald AT, Bekki S, Butchart N, Chipperfield MP, Deushi M, Dhomse SS, Garcia RR, Hardiman SC, Horowitz LW, Jöckel P, Josse B, Kinnison D, Lin M, Mancini E, Manyin ME, Marchand M, Maréchal V, Michou M, Oman LD, Pitari G, Plummer DA, Revell LE, Saint-Martin D, Schofield R, Stenke A, Stone K, Sudo K, Tanaka TY, Tilmes S, Yamashita Y, Yoshida K, Zeng G (2017) Review of the global models used within phase 1 of the Chemistry–Climate Model Initiative (CCMI). *Geoscientific Model Development* 10, 639–671. doi:10.5194/gmd-10-639-2017
- Nadeau D, Doutriaux C, Bradshaw T, Kettleborough J, Weigel T, Hogan E, Durack PJ (2016) PCMDI/cmor: CMOR version 3.2.0. doi:10.5281/zenodo.168253

- Oke PR, Griffin DA, Schiller A, Matear RJ, Fiedler R, Mansbridge J, Lenton A, Cahill M, Chamberlain MA, Ridgway K (2013) Evaluation of a near-global eddy-resolving ocean model. *Geoscientific Model Development* 6, 591–615. doi:10.5194/gmd-6-591-2013
- O'Neill BC, Tebaldi C, van Vuuren DP, Eyring V, Friedlingstein P, Hurtt G, Knutti R, Kriegler E, Lamarque J-F, Lowe J, Meehl GA, Moss R, Riahi K, Sanderson BM (2016) The Scenario Model Intercomparison Project (ScenarioMIP) for CMIP6. *Geoscientific Model Development* 9, 3461–3482. doi:10.5194/gmd-9-3461-2016
- Orr JC, Najjar RG, Aumont O, Bopp L, Bullister JL, Danabasoglu G, Doney SC, Dunne JP, Dutay J-C, Graven H, Griffies SM, John JG, Joos F, Levin I, Lindsay K, Matear RJ, McKinley GA, Mouchet A, Oschlies A, Romanou A, Schlitzer R, Tagliabue A, Tanhua T, Yool A (2017) Biogeochemical protocols and diagnostics for the CMIP6 Ocean Model Intercomparison Project (OMIP). *Geoscientific Model Development* 10, 2169–2199. doi:10.5194/gmd-10-2169-2017
- Otto-Bliesner BL, Braconnot P, Harrison SP, Lunt DJ, Abe-Ouchi A, Albani S, Bartlein PJ, Capron E, Carlson AE, Dutton A, Fischer H, Goelzer H, Govin A, Haywood A, Joos F, LeGrande AN, Lipscomb WH, Lohmann G, Mahowald N, Nehrbass-Ahles C, Pausata FSR, Peterschmitt J-Y, Phipps SJ, Renssen H, Zhang Q (2017) The PMIP4 contribution to CMIP6 – part 2: two interglacials, scientific objective and experimental design for Holocene and Last Interglacial simulations. *Geoscientific Model Development* 10, 3979–4003. doi:10.5194/gmd-10-3979-2017
- Pincus R, Forster PM, Stevens B (2016) The Radiative Forcing Model Intercomparison Project (RFMIP): experimental protocol for CMIP6. *Geoscientific Model Development* 9, 3447–3460. doi:10.5194/gmd-9-3447-2016
- Rashid HA, Sullivan A, Dix M, Bi D, Mackallah C, Ziehn T, Dobrohotoff P, O'Farrell S, Harman IN, Bodman R, Marsland S (2022) Evaluation of climate variability and change in ACCESS historical simulations for CMIP6. *Journal of Southern Hemisphere Earth Systems Science* [Published online 14 July 2022]. doi:10.1071/ES21028
- Rugenstein M, Bloch-Johnson J, Abe-Ouchi A, Andrews T, Beyerle U, Cao L, Chadha T, Danabasoglu G, Dufresne J-L, Duan L, Foujols M-A, Frölicher T, Geoffroy O, Gregory J, Knutti R, Li C, Marzocchi A, Mauritsen T, Menary M, Moyer E, Nazarenko L, Paynter D, Saint-Martin D, Schmidt GA, Yamamoto A, Yang S (2019) LongRunMIP: motivation and design for a large collection of millennial-length AOGCM simulations. *Bulletin of the American Meteorological Society* 100, 2551–2570. doi:10.1175/BAMS-D-19-0068.1
- Savita A, Marsland S, Dix M, Bi D, Dobrohotoff P, Fiedler R, Mackallah C, Sullivan A, Dias FB, Domingues C, Hannah N, Heerdegen A, Hogg A, Druken K (2019) CSIRO-ARCCESS ACCESS-CM2 model output prepared for CMIP6 FAFMIP. doi:10.22033/ESGF/CMIP6.2282
- Sellar AA, Walton J, Jones CG, Wood R, Abraham NL, Andrejczuk M, Andrews MB, Andrews T, Archibald AT, de Mora L, Dyson H, Elkington M, Ellis R, Florek P, Good P, Gohar L, Haddad S, Hardiman SC, Hogan E, Iwi A, Jones CD, Johnson B, Kelley DJ, Kettleborough J, Knight JR, Köhler MO, Kuhlbrodt T, Liddicoat S, Linova-Pavlova I, Mizielinski MS, Morgenstern O, Mulcahy J, Neiningner E, O'Connor FM, Petrie R, Ridley J, Rioual J-C, Roberts M, Robertson E, Rumbold S, Seddon J, Shepherd H, Shim S, Stephens A, Teixeira JC, Tang Y, Williams J, Wiltshire A, Griffiths PT (2020) Implementation of UK earth system models for CMIP6. *Journal of Advances in Modeling Earth Systems* 12, e2019MS001946. doi:10.1029/2019MS001946
- Senior CA, Jones CG, Wood RA, Sellar A, Belcher S, Klein-Tank A, Sutton R, Walton J, Lawrence B, Andrews T, Mulcahy JP (2020) UK community earth system modeling for CMIP6. *Journal of Advances in Modeling Earth Systems* 12, e2019MS002004. doi:10.1029/2019MS002004
- Sherwood SC, Webb MJ, Annan JD, Armour KC, Forster PM, Hargreaves JC, Hegerl G, Klein SA, Marvel KD, Rohling EJ, Watanabe M, Andrews T, Braconnot P, Bretherton CS, Foster GL, Hausfather Z, von der Heydt AS, Knutti R, Mauritsen T, Norris JR, Proistosescu C, Rugenstein M, Schmidt GA, Tokarska KB, Zelinka MD (2020) An assessment of earth's climate sensitivity using multiple lines of evidence. *Reviews of Geophysics* 58, e2019RG000678. doi:10.1029/2019RG000678
- Smith CJ, Kramer RJ, Myhre G, Alterskjær K, Collins W, Sima A, Boucher O, Dufresne J-L, Nabat P, Michou M, Yukimoto S, Cole J, Paynter D, Shiogama H, O'Connor FM, Robertson E, Wiltshire A, Andrews T, Hannay C, Miller R, Nazarenko L, Kirkevåg A, Olivie D, Fiedler S, Lewinschal A, Mackallah C, Dix M, Pincus R, Forster PM (2020) Effective radiative forcing and adjustments in CMIP6 models. *Atmospheric Chemistry and Physics* 20, 9591–9618. doi:10.5194/acp-20-9591-2020
- Storkey D, Blaker AT, Mathiot P, Megann A, Aksenov Y, Blockley EW, Calvert D, Graham T, Hewitt HT, Hyder P, Kuhlbrodt T, Rae JGL, Sinha B (2018) UK Global Ocean GO6 and GO7: a traceable hierarchy of model resolutions. *Geoscientific Model Development* 11, 3187–3213. doi:10.5194/gmd-11-3187-2018
- Taylor K, Williamson D, Zwiers F (2000) AMIP II sea surface temperature and sea ice concentration boundary conditions. PCMDI Report, Vol. 60.
- Thomason LW, Ernest N, Millán L, Rieger L, Bourassa A, Vernier J-P, Manney G, Luo B, Arfeuille F, Peter T (2018) A global space-based stratospheric aerosol climatology: 1979–2016. *Earth System Science Data* 10, 469–492. doi:10.5194/essd-10-469-2018
- Toohey M, Stevens B, Schmidt H, Timmreck C (2016) Easy Volcanic Aerosol (EVA v1.0): an idealized forcing generator for climate simulations. *Geoscientific Model Development* 9, 4049–4070. doi:10.5194/gmd-9-4049-2016
- Tsujino H, Urakawa S, Nakano H, Small RJ, Kim WM, Yeager SG, Danabasoglu G, Suzuki T, Bamber JL, Bentsen M, Böning CW, Bozec A, Chassignet EP, Curchitser E, Boeira Dias F, Durack PJ, Griffies SM, Harada Y, Ilicak M, Josey SA, Kobayashi C, Kobayashi S, Komuro Y, Large WG, Le Sommer J, Marsland SJ, Masina S, Scheinert M, Tomita H, Valdivieso M, Yamazaki D (2018) JRA-55 based surface dataset for driving ocean–sea-ice models (JRA55-do). *Ocean Modelling* 130, 79–139. doi:10.1016/j.ocemod.2018.07.002
- Tsujino H, Urakawa LS, Griffies SM, Danabasoglu G, Adcroft AJ, Amaral AE, Arsouze T, Bentsen M, Bernardello R, Böning CW, Bozec A, Chassignet EP, Danilov S, Dussin R, Exarchou E, Fogli PG, Fox-Kemper B, Guo C, Ilicak M, Iovino D, Kim WM, Koldunov N, Lapin V, Li Y, Lin P, Lindsay K, Liu H, Long MC, Komuro Y, Marsland SJ, Masina S, Nummelin A, Rieck JK, Ruprich-Robert Y, Scheinert M, Sicardi V, Sidorenko D, Suzuki T, Tatebe H, Wang Q, Yeager SG, Yu Z (2020) Evaluation of global ocean–sea-ice model simulations based on the experimental protocols of the Ocean Model Intercomparison Project phase 2 (OMIP-2). *Geoscientific Model Development* 13, 3643–3708. doi:10.5194/gmd-13-3643-2020
- Uhe P, Hume T, Collier M (2012) ACCESS Post-Processor Version 1.0, CAWCR Technical Report Number 058. Available at [https://www.cawcr.gov.au/technical-reports/CTR\\_058.pdf](https://www.cawcr.gov.au/technical-reports/CTR_058.pdf)
- van Marle MJE, Kloster S, Magi BI, Marlon JR, Daniau A-L, Field RD, Arneft A, Forrest M, Hantson S, Kehrwald NM, Knorr W, Lasslop G, Li F, Mangeon S, Yue C, Kaiser JW, van der Werf GR (2017) Historic global biomass burning emissions for CMIP6 (BB4CMIP) based on merging satellite observations with proxies and fire models (1750–2015). *Geoscientific Model Development* 10, 3329–3357. doi:10.5194/gmd-10-3329-2017
- Walters D, Baran AJ, Boutle I, Brooks M, Earnshaw P, Edwards J, Furtado K, Hill P, Lock A, Manners J, Morcrette C, Mulcahy J, Sanchez C, Smith C, Stratton R, Tennant W, Tomassini L, Van Weverberg K, Vosper S, Willett M, Browse J, Bushell A, Carslaw K, Dalvi M, Essery R, Gedney N, Hardiman S, Johnson B, Johnson C, Jones A, Jones C, Mann G, Milton S, Rumbold H, Sellar A, Ujiie M, Whitall M, Williams K, Zerroukat M (2019) The Met Office Unified Model Global Atmosphere 7.0/7.1 and JULES Global Land 7.0 configurations. *Geoscientific Model Development* 12, 1909–1963. doi:10.5194/gmd-12-1909-2019
- Wang YP, Law RM, Pak B (2010) A global model of carbon, nitrogen and phosphorus cycles for the terrestrial biosphere. *Biogeosciences* 7, 2261–2282. doi:10.5194/bg-7-2261-2010
- Watterson IG, Keane RJ, Dix M, Ziehn T, Andrews T, Tang Y (2021) Analysis of CMIP6 atmospheric moisture fluxes and the implications for projections of future change in mean and heavy rainfall. *International Journal of Climatology* 41, E1417–E1434. doi:10.1002/joc.6777
- Woodward S (2011) Mineral dust in HadGEM2. Technical note 87, Hadley Centre.
- Yeung N, Menviel L, Meissner K, Ziehn T, Chamberlain M, Mackallah C, Druken K, Ridzwan SM (2019) CSIRO ACCESS-ESM1.5 model output prepared for CMIP6 PMIP. doi:10.22033/ESGF/CMIP6.13701
- Yeung NK-H, Menviel L, Meissner KJ, Taschetto AS, Ziehn T, Chamberlain M (2021) Land–sea temperature contrasts at the Last Interglacial and their impact on the hydrological cycle. *Climate of the Past* 17, 869–885. doi:10.5194/cp-17-869-2021

- Zelinka MD, Myers TA, McCoy DT, Po-Chedley S, Caldwell PM, Ceppi P, Klein SA, Taylor KE (2020) Causes of higher climate sensitivity in CMIP6 Models. *Geophysical Research Letters* **47**, e2019GL085782. doi:10.1029/2019GL085782
- Zhang Q, Pitman AJ, Wang YP, Dai YJ, Lawrence PJ (2013) The impact of nitrogen and phosphorous limitation on the estimated terrestrial carbon balance and warming of land use change over the last 156 yr. *Earth System Dynamics* **4**, 333–345. doi:10.5194/esd-4-333-2013
- Ziehn T, Chamberlain M, Lenton A, Law R, Bodman R, Dix M, Mackallah C, Druken K, Ridzwan SM (2019a) CSIRO ACCESS-ESM1.5 model output prepared for CMIP6 C4MIP. doi:10.22033/ESGF/CMIP6.2286
- Ziehn T, Chamberlain M, Lenton A, Law R, Bodman R, Dix M, Mackallah C, Druken K, Ridzwan SM (2019b) CSIRO ACCESS-ESM1.5 model output prepared for CMIP6 CDRMIP. doi:10.22033/ESGF/CMIP6.2287
- Ziehn T, Chamberlain M, Lenton A, Law R, Bodman R, Dix M, Wang Y, Dobrohotoff P, Srbinovsky J, Stevens L, Vohralik P, Mackallah C, Sullivan A, O'Farrell S, Druken K (2019c) CSIRO ACCESS-ESM1.5 model output prepared for CMIP6 CMIP. doi:10.22033/ESGF/CMIP6.2288
- Ziehn T, Chamberlain M, Lenton A, Law R, Bodman R, Dix M, Wang Y, Dobrohotoff P, Srbinovsky J, Stevens L, Vohralik P, Mackallah C, Sullivan A, O'Farrell S, Druken K (2019d) CSIRO ACCESS-ESM1.5 model output prepared for CMIP6 ScenarioMIP. doi:10.22033/ESGF/CMIP6.2291
- Ziehn T, Chamberlain MA, Law RM, Lenton A, Bodman RW, Dix M, Stevens L, Wang YP, Srbinovsky J (2020a) The Australian Earth System Model: ACCESS-ESM1.5. *Journal of Southern Hemisphere Earth Systems Science* **70**, 193–214. doi:10.1071/ES19035
- Ziehn T, Dix M, Mackallah C, Chamberlain M, Lenton A, Law R, Druken K, Ridzwan SM (2020b) CSIRO ACCESS-ESM1.5 model output prepared for CMIP6 DAMIP. doi:10.22033/ESGF/CMIP6.14362
- Ziehn T, Dix M, Mackallah C, Chamberlain M, Lenton A, Law R, Druken K, Ridzwan SM (2020c) CSIRO ACCESS-ESM1.5 model output prepared for CMIP6 RFMIP. doi:10.22033/ESGF/CMIP6.2290
- Ziehn T, Lenton A, Law R (2020d) An assessment of land-based climate and carbon reversibility in the Australian Community Climate and Earth System Simulator. *Mitigation and Adaptation Strategies for Global Change* **25**, 713–731. doi:10.1007/s11027-019-09905-1
- Ziehn T, Dix M, Mackallah C, Chamberlain M, Lenton A, Law R, Druken K, Ridzwan SM (2021a) CSIRO ACCESS-ESM1.5 model output prepared for CMIP6 LUMIP. Available at <http://cera-www.dkrz.de/WDCC/meta/CMIP6/CMIP6.LUMIP.CSIRO.ACCESS-ESM1-5>
- Ziehn T, Wang Y-P, Huang Y (2021b) Land carbon-concentration and carbon-climate feedbacks are significantly reduced by nitrogen and phosphorus limitation. *Environmental Research Letters* **16**, 074043. doi:10.1088/1748-9326/ac0e62

**Data availability.** CMORised simulation data are published on the Earth System Grid at [Dix et al. \(2019a\)](#) (ACCESS-CM2), [Ziehn et al. \(2019c\)](#) (ACCESS-ESM1.5), [Hayashida et al. \(2021\)](#) (ACCESS-OM2) and [Holmes et al. \(2021\)](#) (ACCESS-OM2-025). See also <https://esgf.nci.org.au/search/cmip6-nci> (ESGF data portal, NCI node) and <https://doi.org/10.25914/5e6acd0492b39> (NCI GeoNetwork record). NCI users can also access the data directly from project fs38 (<https://my.nci.org.au/mancini/project/fs38>). Model output, the semi-processed simulation data which include many variables not requested by CMIP6, that has not been CMORised is also available for NCI users in project p73 (<https://my.nci.org.au/mancini/project/p73>).

**Conflicts of interest.** Josephine Brown is an Associate Editor for the *Journal of Southern Hemisphere Earth Systems Science* but did not at any stage have editor-level access to this manuscript while in peer review, as is the standard practice when handling manuscripts submitted by an editor to this journal. The authors have no further conflicts of interest to declare.

**Declaration of funding.** ACCESS simulations undertaken with the assistance an Australasian Leadership Computing Grant by sponsor, the National Computational Infrastructure (NCI Australia) (grant #I2840 under ALCG2020, NCI project gy57). NCI Australia had a governance role in the publication of ACCESS data to CMIP6, and NCI staff contributed to the preparation of this manuscript. COSIMA and A. E. Kiss were funded by Australian Research Council grants LP160100073 and LP200100406. A. E. Kiss was also funded by the Australian Government's Australian Antarctic Science Program grant 4541. This research was undertaken with the assistance of resources from the NCI, which is supported by the Australian Government.

**Acknowledgements.** We acknowledge the World Climate Research Programme, which, through its Working Group on Coupled Modelling, coordinated and promoted CMIP6. We thank the Earth System Grid Federation (ESGF) for archiving the data and providing access, and the multiple funding agencies who support CMIP6 and ESGF. The ACCESS CMIP6 submission work was jointly funded through CSIRO and the Earth Systems and Climate Change Hub and subsequent Climate Systems Hub of the Australian Government's National Environmental Science Program (NESP). ACCESS simulations, data processing and data publication were undertaken with the assistance of resources from NCI Australia, a NCRIS-enabled (National Collaborative Research Infrastructure Strategy) capability supported by the Australian Government. We also thank Rui Yang and Paul Leopardi at NCI Australia for their work to enable ACCESS modelling on Raijin and Gadi. The UM software is used under the auspices of a partnership agreement between the UK Met Office, CSIRO and the Australian Bureau of Meteorology. This work was built on the allied research efforts of the host institutions, the ARC Centre of Excellence for Climate Extremes (CLEX) and the Consortium for Ocean–Sea-Ice Modelling in Australia (COSIMA).

#### Author affiliations

<sup>A</sup>CSIRO Oceans and Atmosphere, Aspendale, Vic. 3195, Australia.

<sup>B</sup>CSIRO Oceans and Atmosphere, Battery Point, Tas. 7004, Australia.

<sup>C</sup>School of Geography, Earth and Atmospheric Sciences, The University of Melbourne, Parkville, Vic. 3010, Australia.

<sup>D</sup>Australian Research Council Centre of Excellence for Climate Extremes (CLEX), Sydney, NSW 2052, Australia.

<sup>E</sup>National Computational Infrastructure, Acton, ACT 2601, Australia.

<sup>F</sup>CSIRO Oceans and Atmosphere, Black Mountain, ACT 2601, Australia.

<sup>G</sup>Institute for Marine and Antarctic Studies, University of Tasmania, Hobart, Tas. 7005, Australia.

<sup>H</sup>School of Geosciences, University of Sydney, Camperdown, NSW 2006, Australia.

<sup>I</sup>Research School of Earth Sciences, Australian National University, Acton, ACT 2601, Australia.

<sup>J</sup>Climate Change Research Centre, University of New South Wales, Sydney, NSW 2052, Australia.

<sup>K</sup>The Australian Centre for Excellence in Antarctic Science, University of Tasmania, Hobart, Tas. 7001, Australia.

<sup>L</sup>CSIRO Oceans and Atmosphere, Lindfield, NSW 2070, Australia.

<sup>M</sup>CSIRO Information Management & Technology, Black Mountain, ACT 2601, Australia.